Atmos. Chem. Phys. Discuss., https://doi.org/10.5194/acp-2017-1014
Manuscript under review for journal Atmos. Chem. Phys.
Discussion started: 27 November 2017

Atmospheric Chemistry and Physics Discussions

Phenomenology of summer ozone episodes over the Madrid Metropolitan Area, central Spain

Xavier Querol X.[1], Andrés Alastuey A.[1], Gotzon Gangoiti[2], Noemí Perez[1], Hong K. Lee[3], Heeram R. Eun[3], Yonghee Park[3], Enrique Mantilla E.[4], Miguel Escudero[5], Gloria Titos[1], Lucio Alonso[2], Brice Temime-Roussel[6], Nicolas Marchand[6], Juan R. Moreta, M. Arantxa Revuelta[7], Pedro Salvador [8], Begoña Artíñano[8], Saúl García dos Santos[9], Mónica Anguas[10], Alberto Notario[11], Alfonso Saiz-Lopez[10], Roy M. Harrison[12], Kang-Ho Ahn[3]

[1]Institute of Environmental Assessment and Water Research (IDAEA-CSIC), C/Jordi Girona 18-26, Barcelona, 08034 Spain
[2]Escuela Técnica Superior Ingeniería de Bilbao, Departamento Ingeniería Química y del Medio Ambiente, Universidad del País Vasco UPV/EHU, Urkixo Zumarkalea, S/N, Bilbao, 48013 Spain
[3]Department of Mechanical Engineering, Hanyang University, Ansan 425-791, Republic of Korea
[4]Centro de Estudios Ambientales del Mediterráneo, CEAM, Unidad Asociada al CSIC, Parque Tecnológico C/ Charles R. Darwin, 14 Paterna, Valencia, 46980 Spain
[5] Centro Universitario de la Defensa de Zaragoza, Academia General Militar, Ctra. de Huesca s/n, Zaragoza, 50090 Spain
[6]Aix Marseille Univ, CNRS, LCE, Marseille, France
[7]Agencia Estatal de Meteorología, AEMET, C/ Leonardo Prieto Castro, 8, Madrid, 28071 Spain
[8]Department of Environment, CIEMAT, Joint Research Unit Atmospheric Pollution CIEMAT-CSIC, c/ Avenida Complutense 40, Madrid, 28040 Spain
[9]Centro Nacional de Sanidad Ambiental. Instituto de Salud Carlos III (ISCIII), Ctr Majadahoda a Pozuelo km 2, Majadahonda (Madrid), 28222 Spain
[10]Department of Atmospheric Chemistry and Climate, Institute of Physical Chemistry Rocasolano, CSIC, Madrid, 28006 Spain
[11]University of Castilla-La Mancha, Physical Chemistry Department, Faculty of Chemical Science and Technologies, Ciudad Real, Spain.
[12]National Centre for Atmospheric Science, University of Birmingham, B15 2TT United Kingdom. [+]Also at: Department of Environmental Sciences/Centre for Excellence in Environmental Studies, King Abdulaziz University, Jeddah, Saudi Arabia

Abstract

Various studies have reported that photochemical nucleation of new ultrafine particles (UFP) in urban environments within high insolation regions occurs simultaneously with high ozone (O_3). In this work, we evaluate the atmospheric dynamics leading to summer O_3 episodes in the Madrid Air Basin (Central Iberia) by means of measuring a 3D distribution of concentrations for both pollutants. To this end, we obtained vertical profiles (up to 1200 m, above ground level) using tethered balloons and miniaturised instrumentation at a suburban site located to the SW of the Madrid Metropolitan Area (MMA), Majadahonda site (MJDH) in July 2016. Simultaneously, measurements of an extensive number of air quality and meteorological parameters were carried out at 3 supersites across the MMA. Furthermore, data from O_3-soundings and daily radio-sounding were also used to interpret the atmospheric dynamics.

The results demonstrate the concatenation of venting and accumulation episodes, with relative O_3 lows (venting) and peaks (accumulation) in surface levels. Regardless of the episode type, fumigation of high altitude O_3-rich layers contributes the major proportion of surface O_3 concentrations. Accumulation episodes are characterised by a relatively thinner planetary boundary layer (PBL< 1500 m at midday, lower in altitude than the orographic features), low synoptic winds and the development of mountain breezes along the slope of the Guadarrama Mountain Range (W and NW of MMA, maximum altitude >2400 m). This orographic-

meteorological setting causes the vertical recirculation of air masses and the enrichment of O_3 in the lower tropospheric layers. When the highly polluted urban plume from Madrid is affected by these dynamics, the highest O_x (O_3+NO_2) concentrations are recorded in the MMA.

Vertical O_3 profiles during venting episodes, with marked synoptic winds and a deepening of the PBL reaching >2000 m above sea level, were characterised by an upward gradient in O_3 levels, whereas low-altitude O_3 concentration maxima due to local/regional production were found during the accumulation episodes. The two contributions to O_3 surface levels (fumigation from high altitude strata and local/regional production) require very different approaches for policy actions. In contrast to O_3 vertical top-down transfer, UFP are formed in the lowest levels and are transferred upwards progressively with the growth of the PBL.

Keywords: Ozone, ultrafine particles, photochemical pollution, air quality, vertical profiles.

1. Introduction

The EU Directive 2008/50/EC, amended by Directive 2015/1480/EC, on ambient air quality establishes the need to comply with air quality standards to protect citizens and ecosystems. If these are not met, plans to improve air quality must be implemented. Despite the considerable improvements in air quality during the last decade, non-compliances with the European air quality standards are still reported in most Europe. In particular the limit values for nitrogen dioxide (NO_2), particulate matter (PM10 and PM2.5) and tropospheric ozone (O_3) target value are frequently exceeded. Therefore, in 2013, the National Plan for Air Quality and Protection of the Atmosphere (Plan AIRE) 2013-2016, was drawn up, and approved by the Council of Ministers' Agreement of 12/04/2013.

Measures to effectively reduce NO_2 and PM pollution are relatively easy to identify. However, defining policies for abating O_3, other photochemical pollutants and the secondary components of PM is much more complex.

Photochemical pollution is a subject of great environmental importance in Southern (S) Europe due to its climatic and geographical characteristics. Sub-products of this type of contamination are many, noteworthy tropospheric O_3, secondary PM (nitrate, sulphate and secondary organic compounds), and the generation of new ultra-fine particles (UFP) by nucleation (Gomez-Moreno et al., 2011, Brines et al., 2015).

The abatement of tropospheric O_3 levels in this region is a difficult challenge due to its origin, which may be local, regional or transboundary (Millán et al., 2000 and Millán, 2014), the complexity of the meteorological scenarios leading to severe episodes (Millán et al., 1997, Gangoiti et al., 2001, Dieguez et al., 2009 and 2014 and Millán, 2014), as well as the complexity of the chemical processes that drive its formation and sinks, which are not linear in many cases (Monks et al., 2014, and references therein).

This complex context has led to a lack of 'sufficient' O_3 abatement in Spain and Europe; while for primary pollutants, such as SO_2 and CO, and the primary fractions of PM10 and PM2.5 the improvement has been very evident (EEA, 2016). Thus, the latest air quality assessment for

Europe (EEA, 2016) shows that: i) there has been a tendency for the peak O_3 concentration values to decrease in the recent years, but not sufficiently to meet WHO guidelines and EC standards; and ii) the problem of O_3 episodes is more pronounced in the S than in Northern (N) and Central Europe. Likewise, O_3 levels are higher in rural than in urban areas, both due to the generation process, which requires time from the emission of urban, industrial and biogenic precursors, and the consumption (NO titration) of O_3 that takes place in urban areas. Apart from this EEA report, other recent studies such as EMEP (2016), Escudero et al., (2014), Garcia et al (2014) and Querol et al. (2014 and 2016) also evidenced that there is a general tendency for O_3 to increase in urban areas, including traffic sites, probably due to the greater relative reduction of NO emissions compared to NO_2, and therefore to the lower NO titration effect. It is also found that O_3 levels in the regional background have remained constant over the last 15 years, but acute episodes have been drastically reduced compared to the late 1990s, and these markedly increase during heat waves such as those in summer 2003 and 2015 (EEA, 2016, Diéguez et al., 2009 and 2014 and Querol et al., 2016). A recent study reported that an increase of 30-40% in ambient air O_3 levels along with a decrease of 20-40% in NO_2 from 2007 to 2014 in Madrid, may have led to a large concentration increase of up to 70% and 90% in OH and NO_3 (the main tropospheric oxidants), respectively, thereby changing the oxidative capacity of this urban atmosphere (Saiz-Lopez et al., 2017). We still do not know if this increase is due to a decrease in the effect of NO titration or to the fact that the O_3 formation is by volatile organic compounds (VOCs) dominated.

Intensive research on O_3 pollution has been carried out since the late 1980s in the Western Mediterranean, which has been key to understand the behaviour of this pollutant in Europe, and to establish the current air quality European standards (Millán et al., 1991, 1996a, 1996b, 1996c, 2000, 2002; Millán, 2002; EC, 2002, 2004; Millán and Sanz, 1999; Mantilla et al., 1997; Salvador et al., 1997, 1999; Gangoiti et al., 2001; Stein et al., 2004, 2005; Doval et al., 2012; Castell et al., 2008a, 2008b, 2012; Millán et al., 2014, Escudero et al., 2014). Diéguez et al. (2009 and 2014) described in detail the temporal and spatial variation of O_3 levels in Spain. These studies highlight the low inter-annual variability in regional background stations, as well as the existence of specific areas, such as the Madrid air basin, Northern valleys influenced by the Barcelona urban plume, Puertollano basin or the interior of the Valencian region, where very high O_3 episodes are relatively frequent, and point to urban and industrial hot spots as relevant sources of precursors. Recently, Querol et al. (2016) evidenced that the highest O_3 episodes, with hourly exceedances of the information threshold to the population (180 $\mu g/m^3$) for 2000-2015 occurred mostly around these densely populated or industrialised areas.

Querol et al. (2017) reported that the load of O_3 and precursors from the plume of the metropolitan area of Barcelona contributed decisively to the exceedances of the information threshold in the northern areas of Barcelona during the acute O_3 episodes in July 2015. They also demonstrated that the meteorology associated was very complex, similar to the scenarios reported by Gangoiti et al. (2001), Millán (2014) and Diéguez et al. (2014) for other regions of the Western Mediterranean. Regional transport of O_3 is also very relevant, and that acute O_3 episodes, exceeding the information threshold, were caused by a dominant regional contribution (also with high contributions from local formation recirculated during prior days) to O_3, on top of which an additional smaller local 'fresh' contribution was added. It was also

shown that the vast majority of these exceedances are recorded in the month of July of the respective years.

In addition to the primary emissions, nucleation or new particle formation (NPF) processes give rise to relevant contributions to the urban ambient air UFP concentrations, mostly during photochemical pollution episodes in spring and summer (Brines et al., 2015 and references therein). Ambient conditions favouring urban NPF are high insolation, low relative humidity, available SO_2 and VOCs, as well as low pre-existing particle surface area (low condensation sink), common features that enhance new particle formation events (Kulmala et al., 2004; Kulmala and Kerminen, 2008, Sipilä, et al., 2010, Salma et al., 2016).

In this study, we evaluate the temporal and spatial variability of O_3 (and UFP) in the Madrid city/basin, to investigate the causes of acute summer episodes of both pollutants, and to investigate possible inter-relationships. In a subsequent twin article we will focus on the phenomenology of UFP nucleation episodes linked with these photochemical events. Data on UFP are included in this paper only where they assist in interpreting the behaviour of O_3.

2. Methodology

2.1. The study area

The Madrid air basin and the Madrid Metropolitan Area (MMA) are located in the central plain, or Meseta, of the Iberian Peninsula at around 700 m a.s.l. Regarding the topographic features, the Guadarrama range which runs in the NE-SW direction reaches heights up to 2400 m a.s.l. and is located 40 km north from the MMA. To the S, are the Toledo Mountains which run from E to W (Figure 1). Lower mountains are also located to the NE and E, which are part of the Iberian range. Consequently, the Madrid plain shows a NE-SW channelling of winds, forced by the main mountain ranges, and following the basin of the Tagus River and its tributaries. In particular, the MMA is located to the NE of the river basin and at its right side.

Climatologically, the area is characterised by continental conditions with hot summers and cold winters with both seasons typically being dry. Mean annual precipitation of around 400 mm is mainly concentrated in autumn and spring. The MMA is one of the most densely populated regions in Spain, with more than 5 million inhabitants, including Madrid City and surrounding towns. According to Salvador et al. (2015), the main anthropogenic emissions are dominated by road traffic and residential heating (in winter), with minor contributions from industry and a large airport.

Plaza et al. (1997), Pujadas et al. (2000) and Artíñano et al. (2003) described the major meteorological patterns affecting the dispersion of pollutants in the basin, and their seasonality. For summer, Plaza et al. (1997) concluded that the development of strong thermal convective activity and the influence of the mountain ranges produce characteristic mesoscale re-circulations and the development of a very deep mixing layer (Crespí et al., 1995). These authors report that these re-circulations contribute markedly to the high O_3 episodes recorded in the region. According to Plaza et al (1997) and Diéguez et al. (2009 and 2014) the arrangement of the Guadarrama range favours the early heating of its S slopes that causes a clockwise turning of wind direction from a NE component during the night, towards an E and S during the early morning and midday, and to the SW during the late afternoon thus defining

the north-western sector downwind the city as the prone area for O_3 transport. Night time downslope winds inside the basin induce the observed north-easterlies at lower levels. Influenced by these contributions, the barrier effect of the Guadarrama range against the N and NW (Atlantic) winds, as well as the repeated clockwise circulation described above, cause movement of the urban plume of Madrid across the basin. This meteorological system allows local O_3 formation and transport. Regarding the vertical scale, Plaza et al. (1997) also showed that fumigation from high O_3-rich layers (injected by upslope winds the previous day or days, or transported from other areas outside the Madrid basin) could also contribute to enhance the surface O_3 concentrations across the basin. This was attributed to the upward gradient in concentrations in the lower 1 km of the atmosphere measured in the early morning, and the subsequent mixing across the planetary boundary layer (PBL) at midday. Similar results were found by balloon soundings at the Vic Plain (N Barcelona) by Querol et al. (2017), and by earlier studies of Millán et al. (1991, 1992, 1996a to c, 2000, 2002).

On the other hand, Gómez Moreno et al. (2011) and Brines et al. (2015) reported both intensive summer and winter NPF episodes in the western border of Madrid City often with the simultaneous occurrence of the highest O_3 episodes.

2.2. Monitoring sites and instrumentation

To characterise acute summer episodes of O_3 and UFP and to investigate their possible relationships we devised an intensive field campaign in the MMA. Three measurement supersites in and around Madrid, following a WNW direction, according the previously described dynamics, were deployed in an area where the highest levels of O_3 are usually recorded (Reche et al., 2017 submitted) inside the Madrid basin (Figure 1). Table 1 shows the equipment available at the three following supersites:

- Madrid-CSIC, located at the Spanish National Research Council headquarters. This site is located in central Madrid on the sixth floor of the building of the Instituto de Ciencias Agrarias.
- CIEMAT, located at the Centro de Investigaciones Energéticas Medioambientales y Tecnológicas headquarters, at 4 km in a WNW direction from the CSIC site in a suburban area.
- MJDH-ISCIII, located in the Instituto de Salud Carlos III in Majadahonda, at 15 km in a NW direction from the CSIC site.

At MJDH-ISCIII, a PTR-ToF-MS has been deployed from 04 to 19/07/2017 and provides insights into the O_3 Formation Potential (OFP) of the VOC mixture over the MMA area. The operation procedure of the PTR-ToF-MS and OFP calculation are detailed in Table S1 and Figure S1.

Furthermore, from 11 to 14/07/2016, 28 profiles of pollutant and meteorological parameters up to 1200 m a.g.l. were obtained using tethered balloons and a fast winch system (Figure S1, Tables 2). The instrumentation attached to the balloons is summarised in Table 1. The profiles were performed at the Majadahonda Rugby Course (MJDH-RC Figure 1). The balloons were equipped with a Global Position System (GPS) and as set of the instruments (Figure S3), including:

- A miniaturized CPC (Hy-CPC, Hanyang University) was used to measure number concentration of particles larger than 3 nm (PN_3) with a time resolution of 1 s and a flow rate of 0.125 L/min, using butanol as working fluid (Lee et al., 2014). Previous inter-comparison studies with conventional CPCs have yielded very good results (Minguillón et al., 2015). In this work, we will use the terms UFP and PN3 as equivalents but we measure concentrations between 3 and 1000 nm strictly while UFP is <100 nm. However, 80% of the total particle concentration falls in the range of UFPs.

- A PO3M O_3 monitor (2B Technologies) was used to determine O_3 concentrations. It was calibrated against an ultraviolet spectrometry reference analyser showing good agreement (n=34; $PO3MO_3$=1.1058*$RefO_3$+4.41, R^2=0.93). Concentrations (on 10 s basis) are reported in standard conditions (20 °C and 101.3 kPa) and corrected for the reference method.

In addition to the above instrumentation we obtained the following additional meteorological and air quality data:

- Meteorological data from the CIEMAT meteorological tower (four instrumented levels between surface and 54 m a.g.l.), as well as from several AEMET (Spanish Met Office) standard meteorological stations spread out across the basin: Madrid Airport (40.46°N, 3.56°W, 609 m a.s.l), Colmenar Viejo (40.69°N, 3.76°W, 994 m a.s.l), and El Retiro (in Madrid, 40.40°N, 3.67°W, 667 m a.s.l).

- Hourly data for air pollutants (NO, NO_2, SO_2, O_3, PM10 and PM2.5) supplied by the air quality networks of the city of Madrid, the Regional Governments of Madrid, Castilla la Mancha, Castilla y León, and the EMEP monitoring network, supplied by the National Air Quality Database of the Ministry of the Environment of Spain (MAPAMA).

- High resolution O_3-sounding data performed by AEMET at midday each Wednesday at Madrid Airport.

- High resolution meteorological sounding data obtained each day at 00:00 and 12:00 h local time by AEMET also at Madrid Airport. They were used to estimate the height of the PBL at 12:00 UTC by means of the simple parcel method (Pandolfi et al., 2014).

Hourly averaged wind components were calculated and used in polar plots with hourly PM_1, $PM_{2.5}$, NO_2, O_3, O_X (O_3+NO_2), BC and UFP concentrations, by means of the OpenAir R package (Carslaw and Ropkins, 2012).

3. Results

3.1. Meteorological context

Figure 2 shows the time series of the recorded meteorology, measured at a surface station representative of the conditions in the MMA during the field campaign of July 2016 (El Retiro, in central Madrid). In order to put the field campaign into the context of the more general meteorological situation, the time series is extended backwards to the end of June and forward to the end of July 2016. Figure 2 also shows the corresponding time series of O_3, NO_2 and O_X concentrations in the MMA, demonstrating the occurrence of well-marked peaks alternating with relatively low O_3 and O_x concentrations periods. The intensive field campaign

(11-14/07/2016, marked with a green frame) coincides with a low O_3 interval preceding a higher O_3 period in the last two days red and blue frames in Figure 2 show days in which high resolution O_3 free soundings were performed (red and blue indicate intervals within high and low O_3 respectively).

The AEMET O_3 soundings are represented in Figure 3 together with the maps of the 500 hPa geopotential heights (gph in metres) and the MSLP (mean sea level pressure, in mb) contours at 12:00 UTC obtained from the Climate Forecast System (CFS) reanalysis (Saha et al., 2014) downloaded from http://www.wetterzentrale.de/. The low/high O_3 periods coincide with the 500 hPa gph passage of respectively upper level troughs/ridges over the area, associated with cold/warm deep advection of air masses. Cold advections have usually an Atlantic origin.

The local meteorology during the field campaign was characterized by a progressive drop in T (-4°C in the maximal daily T) and an increase in the early morning RH (+20%), with insolation remaining constant (maxima of 900-950 W/m^2) (Figure 4). During the nocturnal and early morning conditions of the first half of the field campaign (11-12/07/2016), relatively weak northerly winds prevailed at the main meteorological surface stations inside the basin, including CIEMAT in Figure 4, and Retiro and Colmenar in Figure 5. This is probably related with drainage (katabatic) conditions inside the Madrid basin, with a progressive turn to a more synoptic westerly component in the central period of the day, consistent with a convective coupling with the more intense upper level wind. This coupling is also accompanied by an important increase of the wind speed at midday, up to 8 m/s (venting stage), that renewed air masses in the whole basin. During the second half of the campaign, intense and persistent north-easterly winds replaced the westerlies from the evening of 12/07/2016, after the evolution of the upper level trough. In contrast to the previous period, during 13-14/07/2016 night-time and early morning conditions registered more intense NE winds (up to 10 m/s) than at midday, after a decrease in intensity down to calm conditions (1 m/s) during the 12/07 morning facilitating both fumigation from upper levels and local O_3 photochemical production. A weak wind veering to the south was also registered at the mentioned surface stations during the 13/07 afternoon, which lasted only for 3 hours, and which is more characteristic of an O_3 enrichment episode, when the veering lasted longer (Plaza et al., 1997). A progressive decrease of the PBL height (-600 m difference) is observed in the AEMET daily radio-soundings that showed a gradual decrease of the midday PBL height, with 3400, 2200, 1900 and 1600 m a.s.l. from 11 to 14/07/2016, Figure S3). This decrease is also observed in the 12 and 14/07/2017 UFP profiles (Figures 7-9, 11). As will be detailed later these meteorological patterns allow O_3 and UFP to smoothly and progressively accumulate in the basin (Figure 4) during the campaign.

In the vertical dimension, during both high and low O_3 periods analysed here, all the soundings show at midday two well defined layers separated by a temperature inversion marking the limit of the growing convection inside the PBL (Figure 3).

In high O_3 periods (6 and 27/07/2016) we found lower PBL heights (approximately 1300-1500 m a.s.l.), with weak winds from the E or NE (less than 4-5 m/s) or calm conditions. This is consistent with the scheme proposed by Plaza et al., (1997), who also described a rapid evolution of the PBL height up to 2500-3000 m a.s.l. at 15:00 UTC during their field campaigns in the area under “summer anticyclonic conditions”. They also described a morning radiative

surface inversion at around 1000 m a.s.l., which was usually "destroyed 1 hour after dawn", and containing NE winds associated with nocturnal drainage flows at lower levels (following the slope of the Madrid basin). In this context, residual layers containing pollutants processed during the previous day can develop above the stably stratified surface layer during night-time conditions. These pollutants can be transported towards the S by weak north-easterly winds, or either remain stagnant under calm conditions and lead to fumigation and mixing with fresh pollutants emitted at the surface after the destabilization of the surface layer as we evidenced in our profiles. These residual layers are topped by the subsidence anticyclonic inversion (1000-1500 m a.s.l.) according to Plaza et al. (1997).

Conversely, the soundings corresponding to low O_3 periods have in common more elevated PBL heights (2000-2500 m a.s.l) with more intense winds (above 6-7 m/s) that can blow from different sectors: from the NE, on the 13/07/2016 (with intense N-Westerlies blowing in the free troposphere) or from the S-SW as observed on the 29/06/2016 and 20/07/2016. The O_3 sounding on 13/07/2016, a unique day within the field campaign, presents the final stage of a low O_3 period with winds in the free troposphere with a clear NW component while channelled north-easterly winds dominate below 2000 m a.s.l. The decrease of surface temperature observed in Figure 2 during the field campaign, is also consistent with the cold advection associated with the troughing in the 500 hPa heights.

3.2. Surface O_3, O_X and UFP during the field campaign

Figure 4 shows the time series of meteorological parameters (CIEMAT tower), NO_2, NO, O_3, BC and UFP concentrations at Madrid-CSIC, Madrid-CIEMAT and MJDH-ISCIII, as well as at MJDH-RC, for the period 11-15/07/2016. As previously stated, the field campaign was characterised by atmospheric venting conditions with the two latter days being in the transitional period to a more stable anticyclonic episode of increasing O_3. The lowering of the wind speed during diurnal periods and other meteorological features mentioned above favoured the gradual accumulation of pollutants as indicated by the progressive increase of the O_3 maxima at MJDH-ISCIII where the O_3 maximum was reached at 15:00 UTC on 13/07/2016 and at 17:00 UTC on 14/07/2016 (Figure 4). The typical accumulation O_3 cycle for the zone was found only on 13 and 14/07/2016 with a maximum at 14:00 UTC on 13/07/2016 and at 16:00 UTC on 14/07/2016. The two previous days presented a more irregular daily pattern, indicating unstable and atypical situations for July (perturbed conditions with prevalence of the synoptic winds). Furthermore, these meteorological conditions and the high insolation induced the concatenation of nucleation episodes in the basin (with low BC and very high UFP levels at the central hours of the day), such as the one on 13/07/2016 (Figure S5).

From 11 to 12/07/2016 the highest concentrations of O_3 were recorded for W-SW and W winds, and peak UFP (PN_3) concentrations were observed with W, SW, WNW and NE winds; however on 13-14/07/2016 both O_3 and UFP concentrations maximized during calm and NE winds (Figure 6). $PM_{2.5}$ levels were independent of the UFP and O_3 variation, increasing in calm situations in the first two days, and with less variation but with somewhat higher concentrations with NE winds in the last two days (Figure 6).

In Figure S5 the evidence for the occurrence of a NPF episode on 13/07/2016 is shown. Morning-midday UFP bursts were caused by nucleation and growth episodes. As previously

stated, in a twin article we will focus on the phenomenology and the vertical occurrence of these nucleation-growth events.

3.3. Vertical O_3 and UFP profiles during the field campaign

Considering the O_3 profiles in Figure 3, high O_3 concentrations (greater than 70 ppb) can be observed above the PBL, between 3000 and 5000 m a.s.l., which may be related to larger scale transport of pollutants previously uplifted to the mid-troposphere. However, at lower levels (inside the PBL) the higher concentrations correspond to the accumulation days (06 and 27/07/2016). As will be demonstrated in this section, O_3 concentrations within the PBL increase throughout the day under all atmospheric conditions due to fumigation from the residual layer, and new O_3 formation from fresh precursors emitted at night-time and through the day. However, larger increases of O_3 concentrations were registered on poorly ventilated days.

As shown in Figure S2 and Table 2, the vertical profiles for 14/07/2016 were the most complete of the campaign (wind speed was relatively low and this allowed extended measurements along the day), and for that reason we begin with the description on this day.

Figure 7 shows that there is a rapid growth of the PBL between 08:05 and 11:01 h UTC, as deduced from the vertical profile of UFP ($PN_{3\text{-}300}$) concentrations. At the beginning of the measurements the upper limit of the PBL was above 1030 m a.s.l. and in 2 h 40 min it was lifted 400 m (around 2.5 m/min). In this initial period, the vertical profile of O_3 was characterized by a succession of strata of different concentrations, but with a clear tendency to increase towards higher altitudes (around 20 ppb of difference between surface level and 1950 m a.s.l. was observed). The discontinuity of the PBL ceiling reflected in the UFP, T and RH profiles did not seem to affect at all the O_3 profile. In other words, we did not notice accumulation of O_3 layers in the top of the PBL, but a general trend to increase towards the highest altitudes reached with the tethered balloons.

Through the course of the day the profile of concentrations of UFP and O_3 became homogenous in the lowest 1200 m a.g.l. (this being the maximum height reached), and a growth of O_3 concentrations at all altitudes was observed until 16:11 h UTC. This homogenisation and growth of O_3 concentrations in the PBL, caused by intense mixing by convection, resulted in a an uneven growth through the day with an increase of 43 ppb at surface and only 10 ppb at 1900 m a.s.l. (Figure 8).

Figure 9 shows the results from measurements taken at a fixed height (1400-1200 m a.s.l.) made to capture the effect of the growth of the PBL on O_3 and UFP levels. We started at around 700 m a.g.l. at 09:32 UTC with 60 ppb of O_3 and around 6000 #/cm^3. At 10:25 UTC the top of the PBL reached the balloon as deduced from the sharp increase in UFP concentrations (up to 20000 #/cm^3). Meanwhile, O_3 concentrations experimented only a slight decrease suggesting that O_3 fluxes are top down and not bottom up as recorded for UFP. From 16:11 h UTC onwards, a reduction of O_3 levels at lower heights was observed (-50 ppb at surface levels from 15:55 to 17:45 h UTC while at 1900 m a.s.l. levels remained stable, Figure 8).

The first balloon flight on 13/07/2016 was performed at 10:45 UTC because earlier the wind speed was too high (Figure 10). At that time the top of the PBL had developed beyond the maximum height reached with the tethered balloons, so in the profile above 1100 m a.g.l. a

very homogeneous concentration was detected. At this time on 14/07/2016 the upper bound of the PBL was perfectly identifiable in the UFP vertical profile over 700 m a.g.l., thus the growth of the PBL was faster on 13/07/2016 than on 14/07/2016. Similarly to 14/07/2016, the 13/07/2016 O_3 profiles were characterised by a progressive increase of concentrations with height (more accentuated in different strata). The profiles started with concentrations close to 40 ppb O_3 at the surface, and reached 83 ppb at the upper heights. As occurred on 14/07/2016, through the course of the day surface concentrations increased differentially with respect to the upper layers, to almost homogenize concentrations in the whole profile (between 68 and 80 ppb at all heights at 15:00 UTC).

In Figure 11 it can be observed that similar results to those described for UFP profiles on the 14/07/2016 were found on 12/07/2016 (upwards growth of the top of the PBL from the early morning):

- Around 700 m a.g.l. at 07:30 UTC (5000 #/cm^3 surface concentrations, 2000 #/cm^3 at the top of the PBL, and 900 #/cm^3 in the free troposphere).
- Around 900 m a.g.l. at 09:00 UTC (9000, 5000 and 2000 #/cm^3 for the above three levels).
- Above 1200 m a.g.l. (this being the maximum measurement height) at 10:00 UTC (10000 #/cm^3 surface concentrations and 7000 #/cm^3 at 1200 m a.g.l.) and 12:55 y 13:42 h (10000 #/ cm^3 surface concentrations and 20000 #/cm^3 at the maximum height of 900 m a.g.l.).

In the early morning of 12/07/2016 O_3 strata at different heights within the PBL were detected, with concentrations reaching 30 to 55 ppb and higher levels (55 to 65 ppb) at the highest altitude reached. During the 10:00 UTC flight O_3 levels reached 75 ppb at the top level decreasing gradually down to 40 ppb at surface levels. At 12:00 UTC concentrations at the top of the profile reached 87 ppb, 70-75 ppb in the 100-700 m a.g.l. transect and 60 ppb in the lowest 100 m a.g.l., where NO titration and O_3 deposition was more efficient. Thus, the 12/07/2016 profiles again showed a vertical trend characterised by i) higher O_3 concentrations at the highest sounding altitude in the early morning, ii) increase in O_3 concentrations as the morning progressed (more pronounced at low altitudes), and iii) homogenous O_3 concentration along the entire vertical profile, except in the surface layers, where the deposition and titration markedly decreased O_3 levels reached at midday. These vertical trends, with concentrations exceeding 75 ppb O_3 above 100-250 m a.g.l., and a marked decrease down to 60 ppb at surface levels was also evident during the short profiles obtained on 11/07/2016 at 18:28-18:41 UTC (Figure 11).

4. Discussion

According to the O_3-soundings and radio-soundings analysed above, as well as previous evidence described by Plaza et al. (1997) and the surface air quality measurements presented in this study, surface O_3 formation from precursor emissions within the MMA seems to develop in the core of regional processes, modulated by large scale meteorological conditions, distinguishing two types of episodes:

- ACCUMULATION, occurring in stable stagnant conditions and regional accumulation of pollutants (in the sense of Millan et al., 1997, 2000; Gangoiti et al., 2001, Millán, 2014), with high O_3 reserve strata accumulated during the previous day in the residual layer and

associated with fumigation around midday in the following day. The O_3 concentrations are high along the whole atmospheric column, but enriched in the lower section by additional local formation of O_3 within the PBL and transport-recirculation of the urban plume of Madrid around the area. This transport is characterised by a net transport to the NW-N during daytime, after vertical mixing, and to the S and SW during night-time, inside the residual layer and decoupled from a more stable nocturnal surface layer. Typically pollutants accumulate during periods of 2-6 days resulting in a well-marked peak and valley concentration periods that affect background, peri-urban and in-city stations. This is the case for the O_3-soundings of 29/06/2016 (not shown), and particularly 27/07/2016 (Figure 12), or the measurements with captive and free balloons by Plaza et al. (1997) in 1993 and 1994, with very high concentrations of O_3 in the lower atmospheric layers, usually forming a bump in the vertical profile of O_3, below a height of 2000 m a.s.l., easily reachable after daytime convection (Figure 12). As illustrated for 06/07/2017, OFP (Table S1 and Figure S1) may be largely dominated by the carbonyls (mostly formaldehyde and acetaldehyde), followed by aromatic compounds (benzene, boluene, C8 aromatics, C9 aromatics and C10 aromatics) when considering the VOC pool during the morning traffic peaks. The influence of aromatic VOCs on OFP rapidly decreases while the influence of biogenic VOCs (primary and secondary) increase throughthe day resulting in a similar potential influence of biogenic and aromatic VOCs on O_3 formation during accumulation periods, but with an OFP still dominated by carbonyls (see supplementary information for additional supporting material).

- VENTING, occurring in advective atmospheric conditions (in the sense of Millan et al., 1997, 2000; Gangoiti et al., 2001, Millán, 2014) with O_3-soundings characterized by (probably external) contributions from high altitude O_3 strata, and their fumigation on the surface (episodes 11-14/07/2016). There is no accumulation of pollutants above the stable nocturnal boundary layer, if any, because more intense and steady winds are charged to sweep out the local production during the preceding day. OFP contributions of carbonyls (dominating OFP), aromatic and biogenic VOCs did not significantly vary for 13 and 14/07/2017 from what it is described above for 06/07/2017.

As detailed in sections 3.1 and 3.2, with weakening of general atmospheric circulation by the end of the campaign period, O_3 and UFP smoothly and progressively accumulated in the basin (Figure 7). An observed decrease of the PBL depth (up to -1800 m at midday according AEMET radio-soundings during the campaign Figure S4), probably also contributed to the progressive increase of pollutant concentrations through the campaign.

With respect to the vertical variability, the general pattern for UFP (N_3) clearly showed a rapid and marked growth of the PBL in the first hours of daylight (Figure 13). In these early stages of the day, O_3 profiles were characterized by a succession of strata of different concentrations, but with a clear increasing trend towards the higher levels (Figure 13). The discontinuity of the PBL ceiling, reflected in the UFP, temperature and humidity profiles, was not identified as such in the O_3 profiles (Figures 7, 9 and 11). As the day progresses the UFP and O_3 concentration profiles are homogenized and a progressive diurnal growth of O_3 concentrations occurs until 16:00 or 17: 00 UTC (Figure 13) which is observed most clearly at the surface. This vertical variability points to different aspects such as: (i) the relevance of fumigation from high altitude O_3-rich strata; ii) surface titration and deposition of O_3; (iii) surface photochemical generation

of O_3 from precursors (with higher concentrations close to the surface); and (iv) horizontal O_3 and precursor surface transport from the urban plume of Madrid towards MJDH-RC. The upper O_3-rich strata might have an external (to the Madrid basin) origin, or might have been injected regionally at high altitudes on the previous day(s) by the complex re-circulations of air masses already reported by Millán et al. (1997, 2000, 2002); EC (2002 and 2004); Gangoiti (2001), Mantilla et al. (1997), Castells et al. (2008a and b) and Millán (2014) for the W Mediterranean, by McKendry et al. (2000) for other parts of the world; and by Plaza et al (1997), and Diéguez et al. (2007 and 2014) for the Madrid area.

According to the last referenced authors, due to the orientation of the Sierra de Guadarrama (Figure 1) the heating of its S slopes throughout the day forces the wind direction to veer, describing an arc that sweeps the zones to the N of Madrid clockwise, from the W to the NE. Dieguéz et al. (2014) showed that the O_3 maxima are recorded at an intermediate point on this route (El Pardo, Colmenar V., see location in Figures 14 and S6) determined by the wind speed, the initial composition of the urban plume, and the result of photochemical processes on its route from the metropolitan area to tens of kilometres away. In addition, our results and those of Plaza et al. (1997) show that O_3 fumigation from high atmospheric layers decisively contributes to the increases in the surface levels, since surface concentrations during our measurements never exceeded those recorded at the highest altitude reached, and at midday homogeneous O_3 levels are measured across the lower 1.2 km of the PBL. During the whole month of July 2016 the described veering of the urban plume, towards W (MJDH-San Martin de V., see location in Figures 14 and S6) in the early hours, and towards NW, N-NE, and, in some cases E and SE, followed by the decoupling and onset of the nocturnal flow towards SW, seems to be causally associated with the O_3 information threshold exceedances, since the maps of exceedances recorded by the official air quality network follow this spatial and temporal evolution (Figure S6). These plume impacts occur in periods when the O_3 concentration is already high because of accumulation in the air mass from one day to the next which is not completely renewed due to general circulation conditions. The relevance of the latter has been recently demonstrated by Otero et al. (2016) who reported the maximum temperature as the parameter more directly related with high O_3 concentrations in central Europe, whereas in the Mediterranean regions it was a high O_3 concentration recorded with a lag of -24 h.

The differential afternoon-evening decrease of O_3 surface concentrations compared with those found at the top of the flights can be attributed to (i) the lower intensity or weakening of the fumigation processes; (ii) a greater O_3 titration and deposition in the lower PBL; and (iii) the lower photochemical O_3 production after the midday insolation maxima. Thus, this process again demonstrates the relevance of high altitude layers and their fumigation to the surface, in the hours of maximum convection.

Regarding the concentrations of UFP, they were very homogeneous throughout the PBL during the vertical profiles, especially in the hours of maximum convection, showing a marked increase from 11 to 14/07/2016 in the whole depth for all profiles (Figure 13). Thus, on the 12/07/2016, the upper limit of the PBL (marked by a sharp reduction of UFP levels) reached 900-1200 m a.g.l. respectively in the flights conducted at 08:05 and 10:12 UTC (Figure 13). In turn, on the 14/07/2016, the top of the PBL at midday exceeded 1200 m a.g.l. only in the afternoon, being constrained to 300 to 700 m a.g.l. from 08:05 and 10:45 h UTC (also shown in

513 the progressive loss of -1800 m in the midday PBL height from 11 to 14/07/2016, revealed by
514 AEMET radio-soundings).

515 The enhanced convection on the 12/07/2016 probably favoured the dilution of UFP
516 concentrations and reinforced the fumigation of O_3 from upper levels. Conversely, the lower
517 development of the PBL on 14/07/2016 hindered the fumigation of upper O_3 layers, resulting
518 in an opposite temporal trend for O_3 and UFP along the profile. Thus, a weaker development of
519 the PBL might result in the increase of UFP concentrations, even if UFP emission/formation
520 rates did not vary significantly. However, we cannot discard the possibility that this UFP
521 increase on the last day was the result of a higher intensity and duration of the nucleation
522 episodes.

523 Consideration of the evolution of surface O_3 concentrations (as shown in Figure 14, on the 11
524 and 12/07/2016) depicts a double wave: the first peak around midday (11:00-14:00 UTC on the
525 first day, and 12:00-13:00 on the second) and the second one in the afternoon-evening (19-
526 22:00 and 16:00-20:00 UTC, respectively), showing relative peaks (not always, sometimes just
527 a plateau). We interpret that the morning increase of O_3 concentrations is dominated by both
528 local production, still dominated by anthropogenic VOCs (Figure S1), and fumigation of upper
529 levels, with an early maximum when layers above are rich in O_3, which progressively decrease
530 with dilution with surface concentrations. The secondary evening concentration peak
531 corresponds to the advection of a locally enriched O_3 air mass (titration always causes O_3
532 depletion towards nocturnal values). When both processes (morning fumigation and evening
533 advection) are not so strong, O_3 local production results in a more typical diurnal time
534 evolution with a single maximum at 15:00-16:00 UTC on 13-14/07/2016 (Figure 14).

535 The relative importance of the local contribution of the MMA to the O_x concentrations
536 registered in the monitoring stations has also been elucidated by comparing the observations
537 at upwind and downwind locations relative to the city. At this respect, Atazar and Alcobendas
538 (Figure 14) are located downwind for 11 and 12/07/2016 and MJDH and Fuenlabrada are
539 upwind while the opposite occurs for 13 and 14/07/2016. As the urban air mass is transported
540 towards the E and NE during the first two days, a local O_x contribution is superimposed to the
541 background at Atazar and Alcobendas where recorded O_x was the highest in the basin (Figure
542 14). The contrary holds during the next two days, when these sites show lower concentrations
543 than the rest. MJDH and Fuenlabrada show a reversed behaviour, with lower concentrations
544 during the first two days and higher for the last days.

545

546 5. Conclusions

547 The phenomenology of O_3 episodes in the Madrid Metropolitan Area (MMA, Central Iberia)
548 has been characterised. We found that O_3 episodes linked with precursors emitted in the
549 Madrid conurbation are modulated by the complex regional atmospheric dynamics.

550 Vertical profiles (up to 1200 m a.g.l.), obtained using tethered balloons and miniaturised
551 instrumentation in Majadahonda (MJDH), a sub-urban site located on the southwestern flank
552 of the Madrid Metropolitan Area (MMA) during 11-14/07/2016, showed how critical processes
553 developed with altitude. Simultaneously, measurements of a number of air quality and

554 meteorological parameters were carried out at 3 supersites within the MMA, where spatial
555 differences highlight the influence of atmospheric dynamics at different scales.

556 The results presented here confirm prior findings regarding the concatenation of relative low
557 (venting) and high (accumulation) O_3 episodes in summer. In the MAB, during both types of
558 episodes, fumigation of high altitude O_3-rich layers contributes with a relevant proportion to
559 surface O_3 concentrations. Moreover, we propose here a conceptual model shown in Figure
560 15. Particularly, accumulation episodes are activated by a relatively thinner PBL (< 1500 m
561 a.g.l. at midday), low synoptic winds, and the development of anabatic winds along the slope
562 of the Sierra de Guadarrama (W and NW of MAB, with >2400 m a.g.l. peaks). This PBL height,
563 lower than the mountain range, and the development of the mountain breezes cause the
564 vertical recirculation of air masses and the enrichment of O_3 in the lower troposphere as well
565 as the formation of reserve strata that fumigate to the surface as the diurnal convective
566 circulation develops. These atmospheric dynamics account for the occurrence of the high Ox
567 (O_3+NO_2) surface concentrations. During venting episodes with a more intense synoptic wind
568 and the top of the PBL usually reaching >2000 m a.g.l, vertical O_3 profiles were characterised
569 by an upward increase of concentrations, whereas lower altitude O_3 maxima were observed in
570 the accumulation periods. Interestingly, vertical profiles demonstrated that during the study
571 period O_3 fumigation (top-down flow) from upper layers prevailed as a contribution to surface
572 O_3 concentrations, whereas the increase of UFP takes place bottom-up, progressing with the
573 development of the PBL and the occurrence of nucleation and growth episodes occurring
574 within the PBL. Thus, when crossing the boundary of the PBL from the free troposphere
575 increases of UFP concentrations by an order of magnitude and a slight decrease of O_3 levels
576 were registered. This O_3 and UFP vertical distribution through the day is consistent with the
577 existence of an efficient venting mechanism, which is able to sweep out the local production of
578 the day. Thus, there is no accumulation of pollutants above the observed stable nocturnal
579 boundary layer from one day to the next, and new UFP production is added from below the
580 following day. The presence of O_3 enriched layers well above the stable nocturnal boundary
581 layer suggests a remote origin of this pollutant in photochemical processes developed at least
582 the day before away from the Madrid basin.

583 The results obtained in this intensive field campaign can be summarized in the following
584 conclusions and recommendations concerning O_3 abatement policies:

585 • The phenomenology of O_3 episodes in S Europe is extremely complex, mainly due to
586 the close relation between photochemistry processes and mesoscale atmospheric
587 dynamics, requiring, consequently, abatement policies very different to the ones
588 useful for Central Europe, as intensive research has demonstrated in the last decades.

589 • During the highest O_3 (accumulation) episodes, apart from the fumigation contribution
590 (X in Figure 15) to surface O_3 concentrations there is an added fraction of O_3 produced
591 locally or transported horizontally (Y in Figure 15). If sensitivity analyses demonstrate
592 that abatement of specific precursors would have an effect reducing O_3 peaks, the
593 reduction strategies (geographic extension, timing…) to decrease Y and X components
594 are very different, and, in most cases, the X component will dominate in the relative
595 contributions. Thus, probably, structural measures over wider regions would be more
596 effective than episodic tactics that might have a larger effect on the Y component. In

terms of precursors, the OFP analysis carried out at ISCIII site shows that even if anthropogenic emissions may still dominate the O_3 formation through the potential impact of alkenes and alkanes (not measured here) and the high contribution of carbonyls (formaldehyde and acetaldehyde), biogenic emissions must be considered. Biogenic VOC (primary and secondary) and aromatic compounds (C6 to C10) contribute to the same extent to the OFP.

- The meteorological scenarios causing the summer accumulation episodes in the MAB (high temperatures, low synoptic winds and relatively thinner PBL) should be forecast, to drive an effective alert system on the possible occurrence of pollution episodes.
- It is necessary to achieve a more detailed characterisation of O_3 precursors (VOC and biogenic VOCs, BVOCs) in the MAB, especially in the source areas, to effectively predict the photochemical evolution of the plumes, and the main impact areas where O_3 from high altitude layers formed the day(s) before from other precursors fumigates to the surface levels enriched in O_3 and other precursors.
- Sensitivity analyses using modelling techniques will permit simulation of the real situation concerning the O_3 abatement potential but only if the following is achieved in advance: i) reproduce the recirculation cells and other local/regional complex meteorological patterns such as the fumigation processes and the plume transport; ii) include a geographically resolved and accurate emission inventory of O_3 precursors in the source areas; and iii) reproduce the origin of the high altitude O_3 strata from external origins.

The conceptual model described here for O_3 episodes confirming the relevance of the vertical re-circulations that Millan et al (1997, 2000), Gangoiti et al. (2001) and Millán (2014) highlighted, and controlled in this case by specific synoptic conditions the PBL depth, may be also applicable to most S Europe. Thus, Otero et al. (2016) demonstrated that in central Europe the highest temperature is the most statistically related parameter for O_3 episodes, while in S Europe it is the O_3 levels recorded the day before (reflecting re-circulation).

Acknowledgements

The present work was supported by the Spanish Ministry of Agriculture, Fishing, Food and Environment, Madrid City Council and Madrid Regional Government, and by the Ministry of Economy, Industry and Competitiveness and FEDER funds under the project HOUSE (CGL2016-78594-R), and by the Generalitat de Catalunya (AGAUR 2015 SGR33). Part of this research was supported by the Korea Ministry of Environment through "The Eco-Innovation project". The support of the CUD of Zaragoza (project CUD 2016-05), UPV/EHU (UFI 11/47, GIU 16/03), the project PROACLIM CGL2014-52877-R, the City Council of Majadahonda for logistic support and AEMET for providing surface meteorological data, and data from radiosoundings and ozone free-soundings is also acknowledged. We thank Alava Ingenieros, TSI, Solma Environmental Solutions, and Airmodus for their support, and María Díez for her computer support in the treatment of radiosonde data.

6. References

Artíñano B., Salvador P., Alonso D.G., Querol X., Alastuey A., 2003. Anthropogenic and natural influence on the PM10 and PM2.5 aerosol in Madrid (Spain). Analysis of high concentration episodes. Environmental Pollution 125, 453-465.

Brines M., Dall'Osto M., Beddows D.C.S., Harrison R.M., Gómez-Moreno F., Núñez L., Artíñano B., Costabile F., Gobbi G.P., Salimi F., Morawska L., Sioutas C., Querol X., 2015. Traffic and nucleation events as main sources of ultrafine particles in high-insolation developed world cities. Atmos. Chem. Phys. 15, 5929-5945.

Carslaw, D. C. and K. Ropkins, (2012) openair --- an R package for air quality data analysis. Environmental Modelling & Software. Volume 27-28, 52-61.

Castell N., Mantilla E., and Millán M.M., 2008a. Analysis of tropospheric ozone concentration on a Western Mediterranean site: Castellon (Spain). Environmental Monitoring and Assessment, 136, 3-11.

Castell N., Stein A.F., Salvador R., Mantilla E., and Millán M.M., 2008b.The impact of biogenic VOC emissions on photochemical ozone formation during a high ozone pollution episode in the Iberian Peninsula in the 2003 summer season. Advances in Science and Research, 2, 9-15.

Castell N., Tellez L., and Mantilla E., 2012. Daily, seasonal and monthly variations in ozone levels recorded at the Turia river basin in Valencia (Eastern Spain). Environmental Science and Pollution Research, 19, 3461-3480.

Commission EU Directive (EU) 2015/1480 of 28 August 2015 amending several annexes to Directives 2004/107/EC and 2008 /50/EC of the European Parliament and of the Council laying down the rules concerning reference methods, data validation and location of sampling points for the assessment of ambient air quality

Crespí S.N., Artíñano B., Cabal H., 1995. Synoptic classification of the mixed-layer height evolution. Journal of Applied Meteorology, 34, 1668-1677.

Dieguez J.J., Calatayud V., Mantilla E., 2014. CEAM Report for the Ministry of Agriculture, Food and Environment, Fundación Biodiversidad. Informe Final. Memoria Técnica Proyecto CONOZE. CONtaminación por OZono en España. 137 pp http://www.magrama.gob.es/es/calidad-y-evaluacion-ambiental/temas/atmosfera-y-calidad-del-aire/Informe_t%C3%A9cnico_CONOZE%5B1%5D_tcm7-330956.pdf

Dieguez J.J., Millán M., Padilla L., Palau J.L., 2009. Estudio y evaluación de la contaminación atmosférica por ozono troposférico en España. CEAM Report for the Ministry of Agriculture, Food and Environment, INF FIN/O3/2009. 372 pp. http://www.magrama.gob.es/es/calidad-y-evaluacion-ambiental/temas/atmosfera-y-calidad-del-aire/8_A_Informe_final_ozono-ceam_Julio_2009_tcm7-152609.pdf

Directive 2008/50/EC of the European Parliament and of the council of 21 May 2008 on ambient air quality and cleaner air for Europe

Doval M., Castell N., Téllez L., and Mantilla E., 2012.The use of experimental data and their uncertainty for assessing ozone photochemistry in the Eastern Iberian Peninsula. Chemosphere 89, 796-804.

EC, 2002. Ozone dynamics in the Mediterranean Basin: A collection of scientific papers resulting from the MECAPIP, RECAPMA and SECAP Projects. Air Pollution Report 78. DG RTD I.2, LX 46 2/82, B-1049 Brussels.

EC, 2004. European Commission Decision of 19 March 2004 “Concerning guidance for implementation of Directive 2002/3/EC of the European Parliament and the Council relating to

ozone in ambient air (2004/279/EC). Official Journal of the European Union L87/50 of 25.3.2004.

EEA, 2016. Air quality in Europe-2016 report. EEA Report, No 28/2016. ISBN 978-92-9213-824-0, Luxembourg: Publications Office of the European Union, 88 pp.

EMEP, 2016. Air pollution trends in the EMEP region between 1990 and 2012. EMEP/CCC-Report 1/2016, ISBN : 978-82-425-2834-6, 107 pp.

Escudero M., Lozano A., Hierro J., del Valle J., Mantilla E., 2014. Urban influence on increasing ozone concentrations in a characteristic Mediterranean agglomeration. Atmospheric Environment 99, 322–332.

Gangoiti G., Millán M.M., Salvador R., and Mantilla E., 2001.Long-range transport and re-circulation of pollutants in the western Mediterranean during the project Regional Cycles of Air Pollution in the West-Central Mediterranean Area. Atmospheric Environment 35, 6267-6276.

Garcia Dos Santos S., Benarroch Benarroch R., Fernández Patier R., Sintes Puertas M.A., Cantón Gálvez J.M., Alonso Herreros J. y Guevara Hernández S. 2014. Atmospheric Pollution in North Africa. Facts and lessons in the Spanish City of Ceuta. 9TH International Conference on Air Quality Science and Application. Garmish (Germany) March 24 – 28.

Gómez-Moreno F.J., Pujadas M., Plaza J., Rodríguez-Maroto J.J., Martínez-Lozano P., Artíñano B., 2011. Influence of seasonal factors on the atmospheric particle number concentration and size distribution in Madrid, Atmos. Environ. 45, 3199-3180.

Kulmala M., Pirjola L., Mäkelä J.M. Stable Sulphate Clusters as a Source of New Atmospheric Particles; Nature 2000, 404, 66-69.

Kulmala M., Vehkamehk H., Pet P.T., Dal Maso M., Lauri A., Kerminen V.-M., Birmili W., McMurry P., 2004. Formation and growth rates of ultrafine atmospheric particles: a review of observations. J. Aerosol Sci. 35, 143-176.

Kulmala M. and Kerminen V.M, 2008. On the formation and growth of atmospheric nanoparticles, Atmos. Research 90, 132-150.

Lee, H.-K., Hwang, I.-K., Ahn, K.-H., 2014. Development and Evaluation of Hy-CPC. Particle and Aerosol Research 10, 93-97.

Mantilla E., Millán M.M., Sanz M.J., Salvador R., and Carratalá A., 1997. Influence of mesometeorological processes on the evolution of ozone levels registered in the Valencian Community. In: I Technical workshop on ozone pollution in southern Europe. Valencia.

McKendry I.G., Lundgren J., 2000. Tropospheric layering of ozone in regions of urbanized complex and/or coastal terrain: a review. Progress in Physical Geography 24, 3.

Millán M.M., 2002. Ozone dynamics in the Mediterranean basin. A collection of scientific papers resulting from the MECAPIP, RECAPMA and SECAP Projects. Air Pollution Research Report 78.Fundación Centro de Estudios Ambientales del Mediterráneo - CEAM. Valencia, España. 287 pp.

Millán, M.M. 2014. Extreme hydrometeorological events and climate change predictions in Europe. J. Hydrol. 518B, 206-224.

Millán M.M., Artiñano B., Alonso L., Navazo M., Castro M., 1991. The effect of meso-scale flows on regional and long-range atmospheric transport in the Western Mediterranean area. Atmospheric Environment 25A, 5/6, 949-963.

Millán, M.; Artíñano B. 1992. Mesometeorological Cycles of Air Pollution in the Iberian Peninsula; Air Pollution Research Report 44, EUR14834; Commission of the European Communities.

Millán M.M., Salvador R., Mantilla E., Artiñano B., 1996a. Meteorology and photochemical air pollution in southern Europe: experimental results from EC research projects. Atmospheric Environment, 30, 1909-1924.

Millán M.M., Mantilla E., Salvador R., Kallos G., 1996b.Regional and long-range transport scenarios for photo-oxidants on the Mediterranean basin in summer. Ninth joint conference on applications of air pollution meteorology. 438-441. American Meteorological Society, Boston.

Millán M.M., Salvador R., Mantilla E., 1996c.Mesoscale processes and photo-oxidants cycles on the Spanish Mediterranean coast. Ninth joint conference on applications of air pollution meteorology.434-437. American Meteorological Society, Boston.

Millán M.M., Salvador R., Mantilla E., and Kallos G., 1997.Photooxidant dynamics in the Mediterranean basin in summer: Results from European research projects. Journal of Geophysical Research 102, 8811-8823.

Millán M.M. and Sanz M. J., 1999. Ozone in Mountainous regions and in Southern Europe. In: Ad hoc Working group on Ozone Directive and Reduction Strategy Development, (eds.). Ozone Position Paper.145-150. European Commission, Brussels.

Millán M.M., Mantilla E., Salvador R., Carratalá A., Sanz M.J., Alonso L., Gangoiti G., and Navazo M., 2000. Ozone Cycles in the Western Mediterranean Basin: Interpretation of Monitoring Data in Complex Coastal Terrain. Journal of Applied Meteorology, 39: 487-508.

Millán M.M., Sanz M.J., Salvador R., and Mantilla E., 2002. Atmospheric dynamics and ozone cycles related to nitrogen deposition in the western Mediterranean. Environmental Pollution, 118, 167-186.

Minguillón M.C., Brines M., Pérez N., Reche C., Pandolfi M., Fonseca A.S., Amato F., Alastuey A., Lyasota A., Codina B., Lee H.-K., Eun H.-R., Ahn K.-H., Querol X., 2015. New particle formation at ground level and in the vertical column over the Barcelona area. Atmospheric Research 164–165, 118–130.

Monks P.S., Archibald A.T., Colette A., Cooper O., Coyle M., Derwent R., Fowler D., Granier C., Law K.S., Mills G.E., Stevenson D.S., Tarasova O., Thouret V., von Schneidemesser E., Sommariva R., Wild O., Williams M.L., 2015. Tropospheric ozone and its precursors from the urban to the global scale from air quality to short-lived climate forcer. Atmos. Chem. Phys., 15, 8889-8973.

Otero N., Sillmann J., Schnell J.L., Rust H., Butler T., 2016. Synoptic and meteorological drivers of extreme ozone concentrations over Europe. Environ. Res. Lett. 11, 024005.

Pandolfi M., Tobías A., Alastuey A., Sunyer J., Schwartz J., Lorente J., Pey J., Querol X., 2014. Effect of atmospheric mixing layer depth variations on urban air quality and daily mortality during Saharan dust outbreaks. Sci. Total Environ., 494-495, 283-289.

Plaza J., Pujadas M., Artíñano B., 1997. Formation and Transport of the Madrid Ozone Plume. J. Air & Waste Manage. Assoc. 47, 766-774.

Pujadas M., Plaza J., Terés J., Artíñano B., Millán M. Passive remote sensing of nitrogen dioxide as a tool for tracking air pollution in urban areas: the Madrid urban plume, a case of study. Atmospheric Environment, 34, 3041-3056.

769 Querol X., Alastuey A., Pandolfi M., Reche C., Pérez N., Minguillón M.C., Moreno T., Viana M.,
770 Escudero M., Orio A., Pallarés M. and Reina F., 2014, '2001–2012 trends on air quality in Spain',
771 Science of the Total Environment 490, 957–969.

772 Querol X., Alastuey A., Orio A., Pallares M., Reina F., Dieguez JJ., Mantilla E., Escudero M.,
773 Alonso L., Gangoiti G., Millán M., 2016. On the origin of the highest ozone episodes in Spain.
774 Science of the Total Environment, 572, 379-389.

775 Querol X., Gangoiti G., Mantilla E., Alastuey A., Minguillón M. C., Amato F., Reche C., Viana M.,
776 Moreno T., Karanasiou A., Rivas I., Pérez N., Ripoll A., Brines M., Ealo M., Pandolfi M., Lee H.-K.,
777 Eun H.-R., Park Y.-H., Escudero M., Beddows D., Harrison R.M., Bertrand A., Marchand N.,
778 Lyasota A., Codina B., Olid M., Udina M., Jiménez-Esteve B., Soler M.R., Alonso L., Millán M.,
779 Ahn, K.-H., 2017. Phenomenology of high-ozone episodes in NE Spain. Atmos. Chem. Phys. 17,
780 2817-2838

781 Reche et al., 2017. On the complexity of Spatial and time dependence of high ozone events in
782 central Spain. Atmospheric Research, submitted.

783 Saha, S.; S. Moorthi, X. Wu, J. Wang, S. Nadiga, P. Tripp, D. Behringer, Y. T. Hou, H. Y. Chuang,
784 M. Iredell, M. Ek, J. Meng, R. Yang, M. Peña Mendez, , H. van den Dool, Q. Zhang, W. Wang, M.
785 Chen, and E. Becker, 2014: The NCEP Climate Forecast System Version 2. Journal of Climate,
786 27, 2185–2208.

787 Saiz-Lopez, A., Borge, R., Notario, A., Adame, J.A., De la Paz, D., Querol, X., Artíñano, B.,
788 Gomez-Moreno, F.J., Cuevas, C.A.: Unexpected increase in the oxidation capacity of the urban
789 atmosphere of Madrid, Spain, Sci. Rep., 7, 45956, doi:10.1038/srep45956, 2017.

790 Salma I, Németh Z, Kerminen V-M, Aalto P, Nieminen T, Weidinger T, Molnár Á, Imre K,
791 Kulmala M., 2016. Regional effect on urban atmospheric nucleation, Atmospheric Chemistry
792 and Physics 16, 8715-8728.

793 Salvador R., Millán M.M., Mantilla E., and Baldasano J.M., 1997.Mesoscale modelling of
794 atmospheric processes over the western Mediterranean area during summer. International
795 Journal of Environment and Pollution, 8, 513-528.

796 Salvador R., Millán M.M., Calbo J., 1999.Horizontal Grid Size Selection and its influence on
797 Mesoscale Model Simulations. Journal of Applied Meteorology, 38, 1311-1329.

798 Salvador P., Artíñano B., Viana M., Alastuey A., Querol X., 2015. Multicriteria approach to
799 interpret the variability of the levels of particulate matter and gaseous pollutants in the
800 Madrid metropolitan area, during the 1999-2012 period. Atmospheric Environment 109, 205-
801 216.

802 Sipilä M., Berndt T., Petäjä T., Brus D., Vanhanen J., Stratmann F., et al. 2010. The role of
803 sulfuric acid in atmospheric nucleation. Science, 327, 5970, 1243-1246.

804 Skrabalova L., Zikova N., Zdimal V., 2015. Shrinkage of newly formed particles in an urban
805 environment. Aerosol Air Qual. Res. 15, 1313-1324.Stanier C.O., Khlystov A.Y., Pandis S.N.,
806 2004. Nucleation events during the Pittsburgh air quality study: description and relation to key
807 meteorological, gas phase, and aerosol parameters. Aerosol Sci. Tech. 38, 253-264.

808 Stein A.F., Mantilla E., and Millán M.M., 2004.Ozone formation downwind an industrial
809 complex in the western Mediterranean. In: 13th World Clean Air and Environmental
810 Protection. August 22-27. London, U.K.

811 Stein A.F., Mantilla E., and Millán M.M., 2005. Using measured and modelled indicators to
812 assess ozone-NOx-VOC sensitivity in a western Mediterranean coastal environment.
813 Atmospheric Environment, 39: 7167-7180.

FIGURES AND TABLES

Figure Captions

Figure 1. Location of the study area, profiles showing the major orographic patterns and location of three supersites (CSIC, CIEMAT, ISCIII) and the site were vertical profile measurements were carried out (MJDH).

Figure 2. Top: Hourly meteorological parameters recorded at El Retiro air quality monitoring station in central Madrid (from 28/06/2016 to 01/08/2016). Middle: Hourly concentrations of O_3 and O_X (O_3+NO_2) recorded at a selection of air quality monitoring station representing the Greater Madrid area, together with those from the remote background station of Campisábalos. Bottom: Hourly NO_2 concentrations recorded at the same sites for the same period. Periods with available AEMET free-soundings of O_3 are bracketed with red (accumulation) or blue (venting) squares. The vertical O_3 and UFP profiling campaign is marked with a green square.

Figure 3: Left: Climate Forecast System Reanalysis (CFSR) for the 500 hPa geopotential heights (gpdams) and mean sea level pressure (MSLP) contours (hPa) at 12:00 UTC in July 2016 (Wetterzentrale, http://www.wetterzentrale.de/), simultaneous with Right: AEMET O_3-free soundings at Madrid airport.

Figure 4. Variation of meteorological parameters (temperature, relative humidity, solar radiation and wind speed and direction), and levels of NO_2, NO, O_3, PM2.5, PM1, BC and UFP (with lower detection limits of 1, 3 and 7 nm, PN_1, PN_3 and PN_7) measured at Madrid-CSIC, Madrid-CIEMAT and ISCIII, as well as in MJDH-RC from 11 to 14/07/2016.

Figure 5. Wind roses for Madrid-CIEMAT and AEMET (El Retiro and Colmenar Viejo stations) and location of the vertical profiling site (MJDH-RC).

Figure 6. Polar plots of the concentrations of hourly O_3 (upper), UFP (PN_3, medium) and PM2.5 (lower) concentrations measured at Madrid-CSIC, Madrid-CIEMAT and MJDH-ISCIII from 11 to 14/07/2016. Wind data used in all cases is the one from the CIEMAT meteorological tower.

Figure 7. Vertical profiles of levels of O_3, UFP (PN_3), temperature and relative humidity obtained on 14/07/2016 (8:05 to 17:45 UTC). A: Ascending; D: Descending.

Figure 8. Vertical profiles of levels of O_3, UFP (PN_3), temperature and relative humidity obtained on 14/07/2016 (8:05 to 17:45 UTC), showing a top-down growth of differential O_3 concentrations from 08:05 with respect those from 15:55 UTC, as well as a bottom up decrease of this differential concentration between 15:55 and 17:45 UTC. A: Ascending; D: Descending.

Figure 9. UFP (PN_3) concentrations for different vertical profiles obtained on 14/07/2016, as well as O_3 and UFP during two periods focusing to evaluate changes produced in a fixed height when reached by the growth of the PBL.

Figure 10. Vertical profiles of levels of O_3, UFP (PN_3), temperature and relative humidity obtained on 13/07/2016 between 10:45 and 15:06 UTC. A: Ascending; D: Descending.

853 Figure 11. Vertical profiles of levels of O_3, UFP (PN_3), temperature and relative humidity
854 obtained on 12 and 11/07/2016. A: Ascending; D: Descending.

855 Figure 12. Top: Vertical profiles of O_3 levels, and temperature obtained on 12/07/1994 (with
856 free sounding) and 15/07/1993 (with tethered balloons). Data obtained from Plaza et al
857 (1997). Bottom: Vertical profiles of O_3 levels of the free soundings by AEMET at Madrid airport
858 (26.6 km east of MJDH-RC) in 06-07/2017.

859 Figure 13. 11-14/07/2017 profiles of O_3 and UFP (PN_3) grouped by hourly stretches from
860 morning to afternoon.

861 Figure 14. Time evolution of hourly O_X (O_3+NO_2) and O_3 concentrations from 11 to 14/07/2016
862 at selected air quality monitoring sites of the Madrid Basin and an external reference site
863 (Campisábalos), as well as the locations of these monitoring sites.

864 Figure 15. Conceptual model of the venting and accumulation O_3 episodes in the Madrid Air
865 Basin, their associated vertical O_3 profiles and the X (fumigation from upper layers) and Y
866 (local/regional) contributions to surface O_3 concentrations in the accumulation episodes.

Atmos. Chem. Phys. Discuss., https://doi.org/10.5194/acp-2017-1014
Manuscript under review for journal Atmos. Chem. Phys.
Discussion started: 27 November 2017

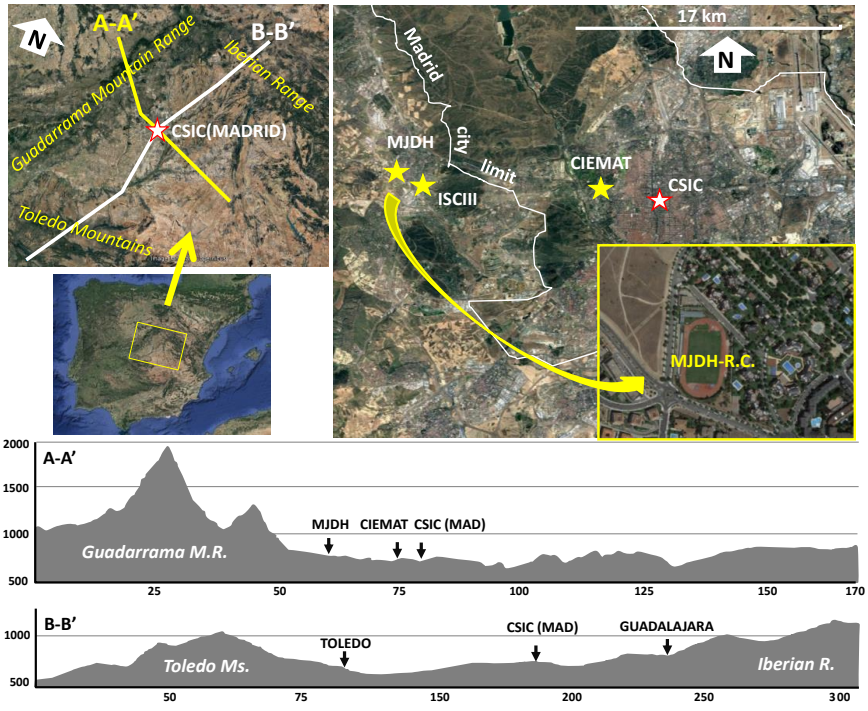

Figure 1

Atmos. Chem. Phys. Discuss., https://doi.org/10.5194/acp-2017-1014
Manuscript under review for journal Atmos. Chem. Phys.
Discussion started: 27 November 2017

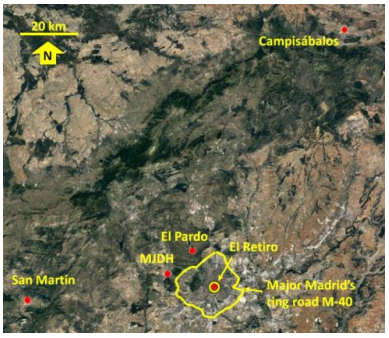

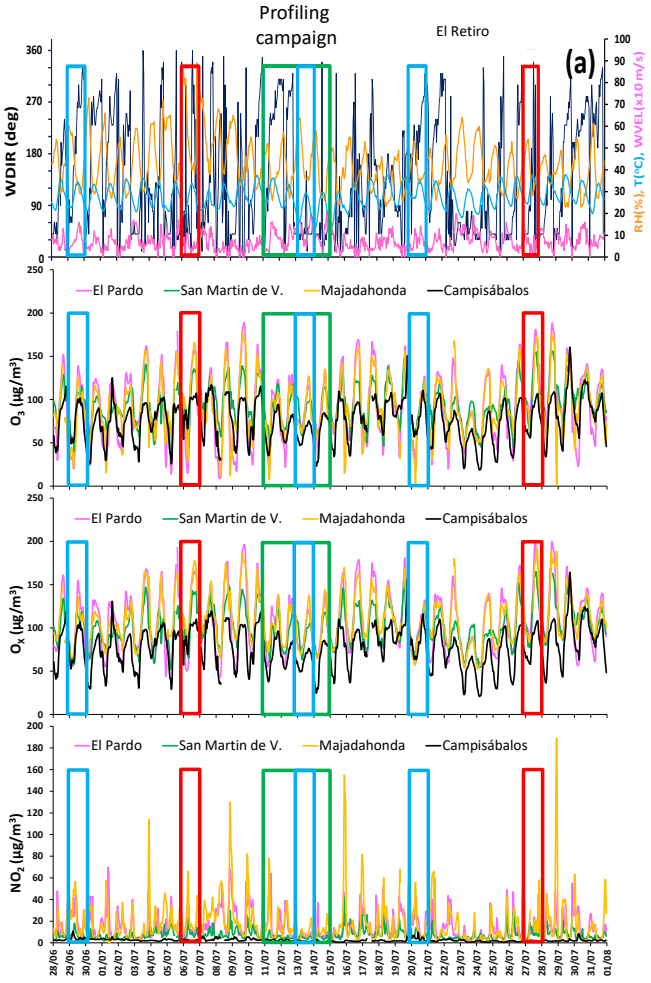

Figure 2

Atmos. Chem. Phys. Discuss., https://doi.org/10.5194/acp-2017-1014
Manuscript under review for journal Atmos. Chem. Phys.
Discussion started: 27 November 2017

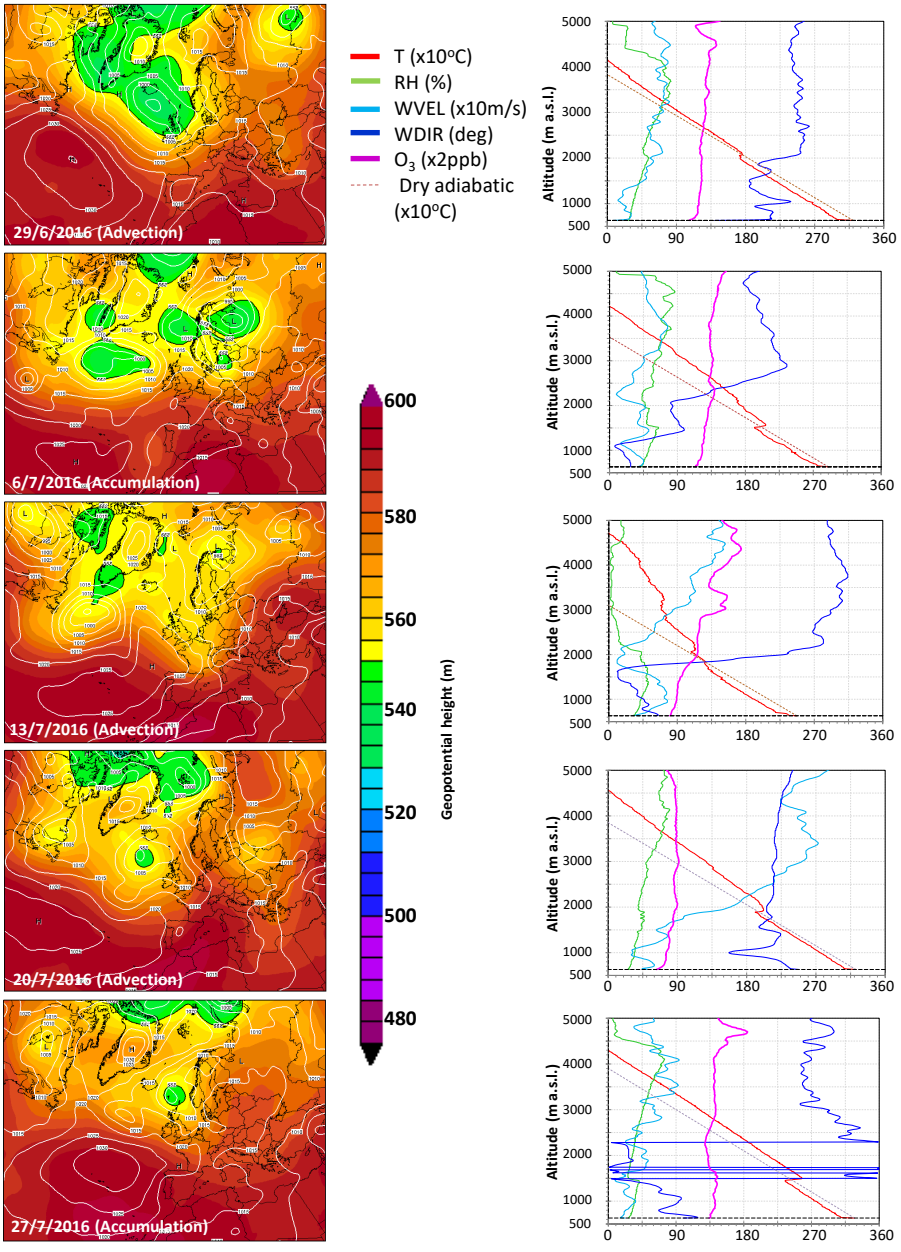

Figure 3

Atmos. Chem. Phys. Discuss., https://doi.org/10.5194/acp-2017-1014
Manuscript under review for journal Atmos. Chem. Phys.
Discussion started: 27 November 2017

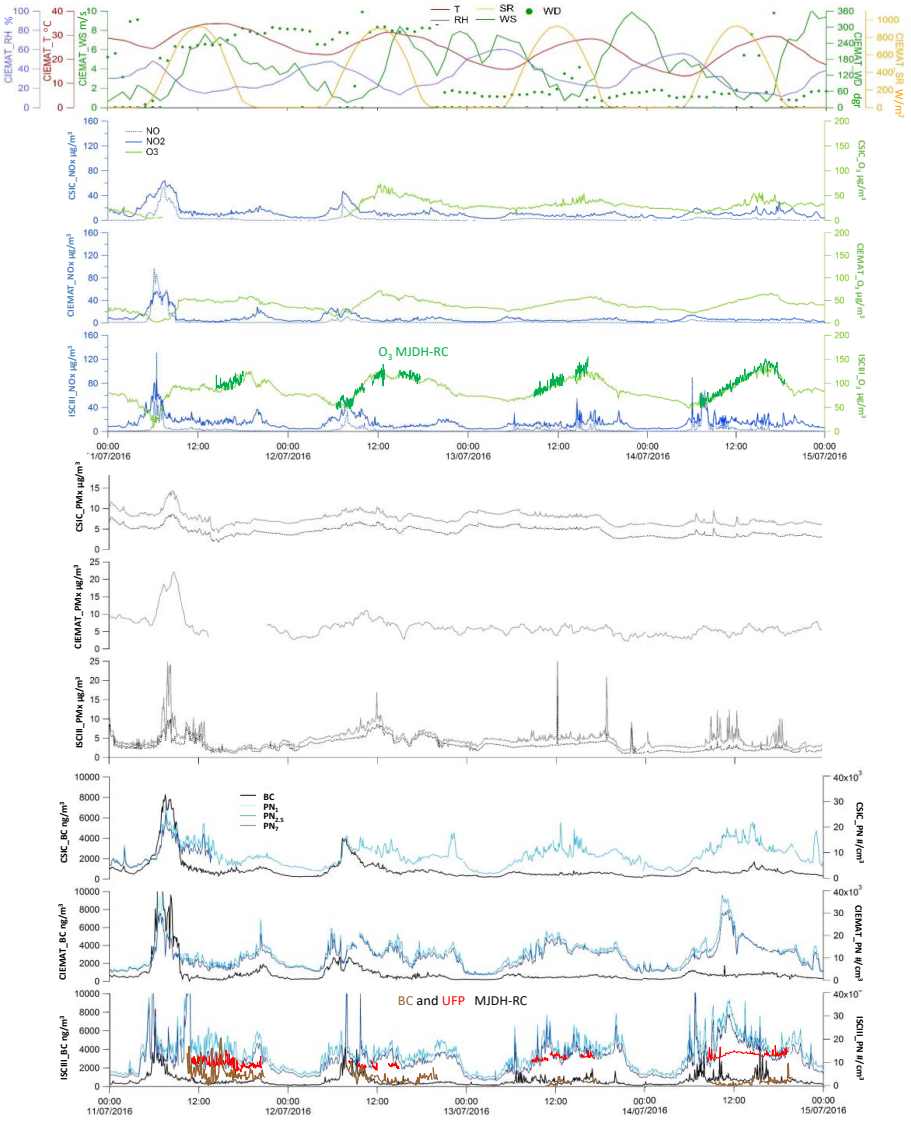

Figure 4

Atmos. Chem. Phys. Discuss., https://doi.org/10.5194/acp-2017-1014
Manuscript under review for journal Atmos. Chem. Phys.
Discussion started: 27 November 2017

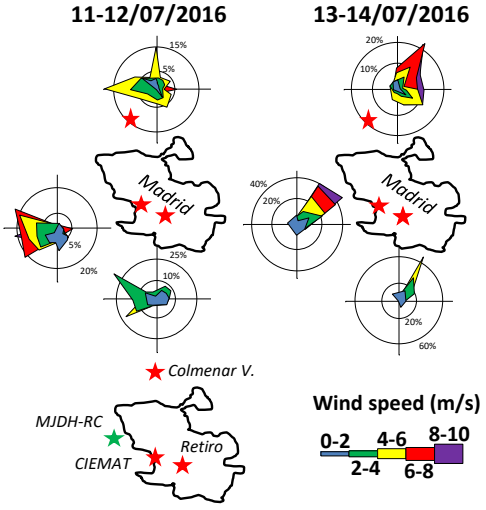

Figure 5.

Atmos. Chem. Phys. Discuss., https://doi.org/10.5194/acp-2017-1014
Manuscript under review for journal Atmos. Chem. Phys.
Discussion started: 27 November 2017

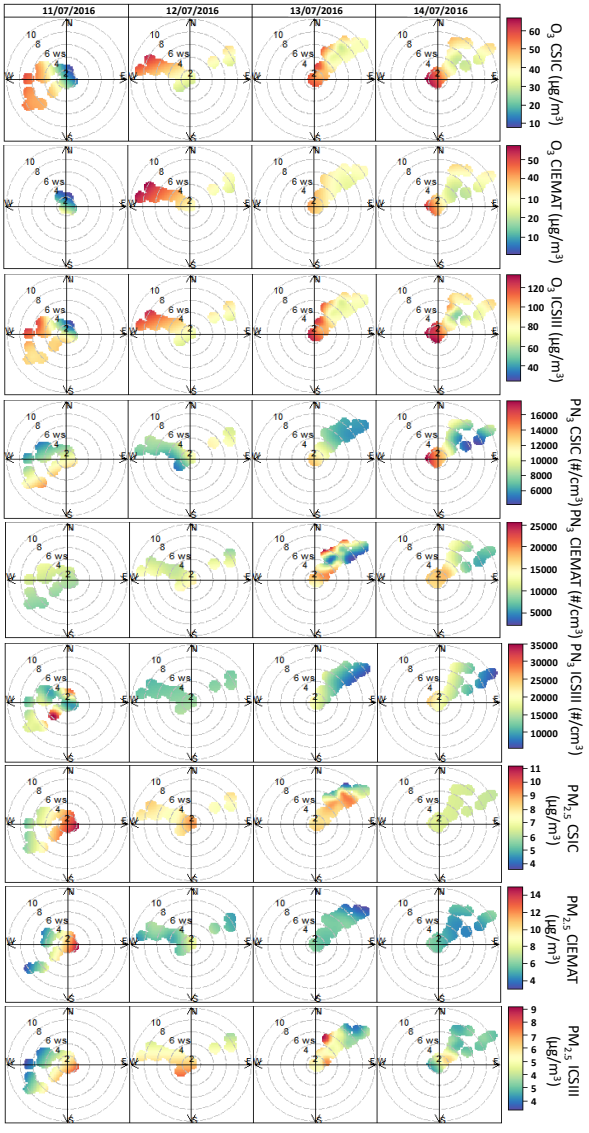

Figure 6

Atmos. Chem. Phys. Discuss., https://doi.org/10.5194/acp-2017-1014
Manuscript under review for journal Atmos. Chem. Phys.
Discussion started: 27 November 2017

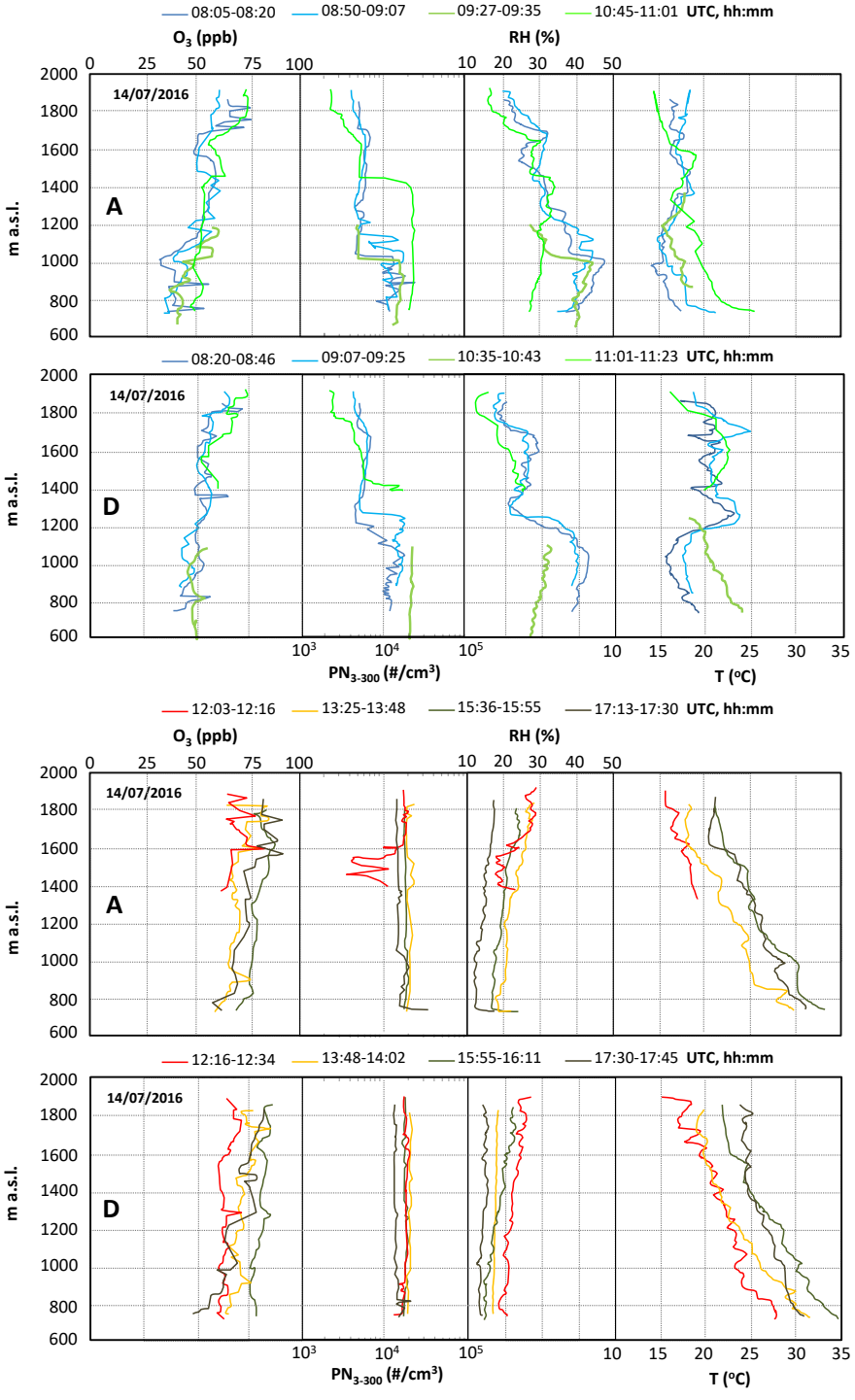

885
886

Figure 7

Atmos. Chem. Phys. Discuss., https://doi.org/10.5194/acp-2017-1014
Manuscript under review for journal Atmos. Chem. Phys.
Discussion started: 27 November 2017

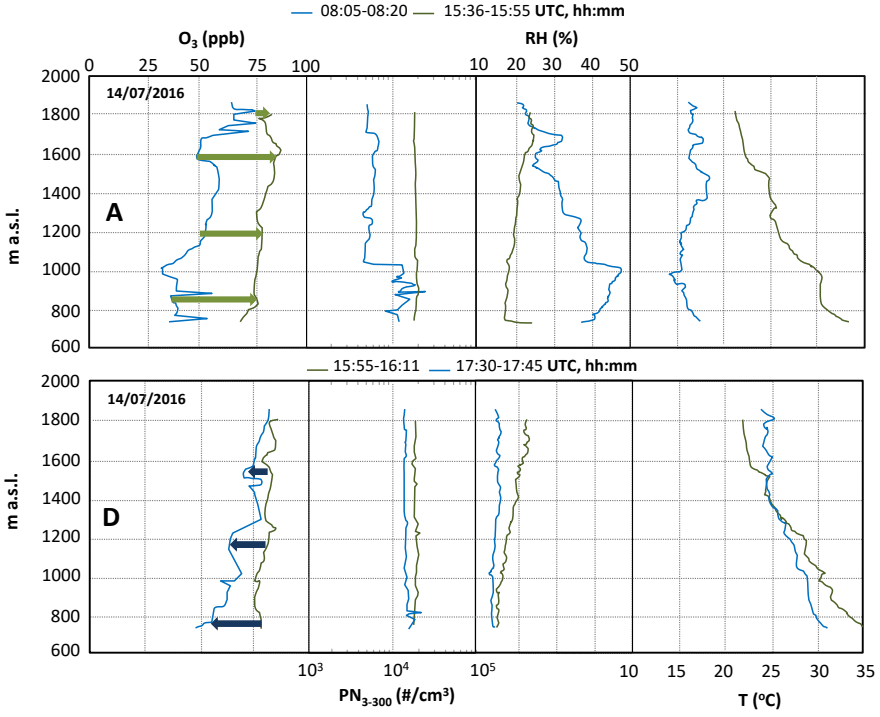

Figure 8

Atmos. Chem. Phys. Discuss., https://doi.org/10.5194/acp-2017-1014
Manuscript under review for journal Atmos. Chem. Phys.
Discussion started: 27 November 2017

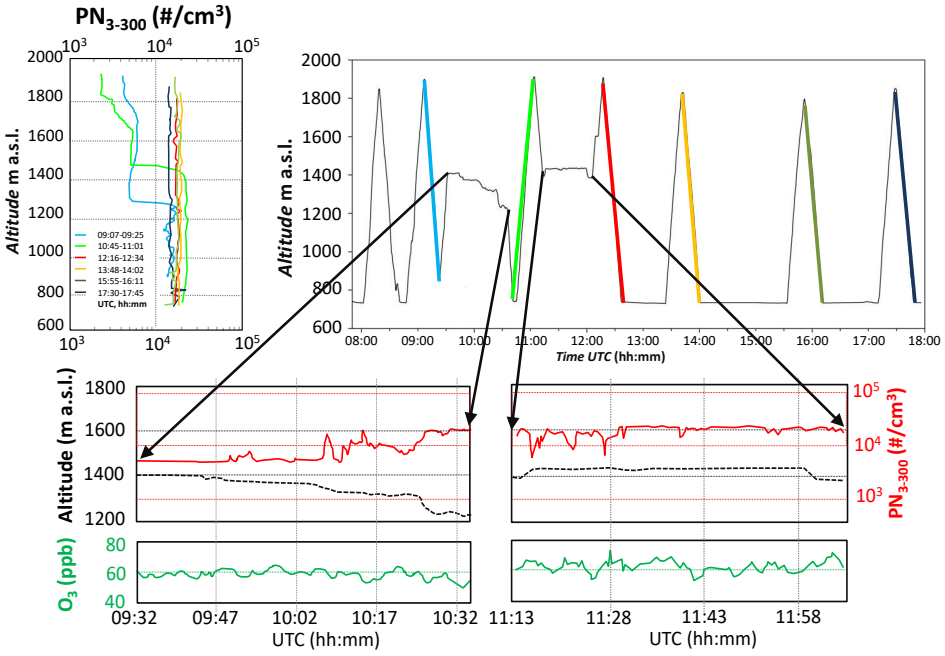

Figure 9

Atmos. Chem. Phys. Discuss., https://doi.org/10.5194/acp-2017-1014
Manuscript under review for journal Atmos. Chem. Phys.
Discussion started: 27 November 2017

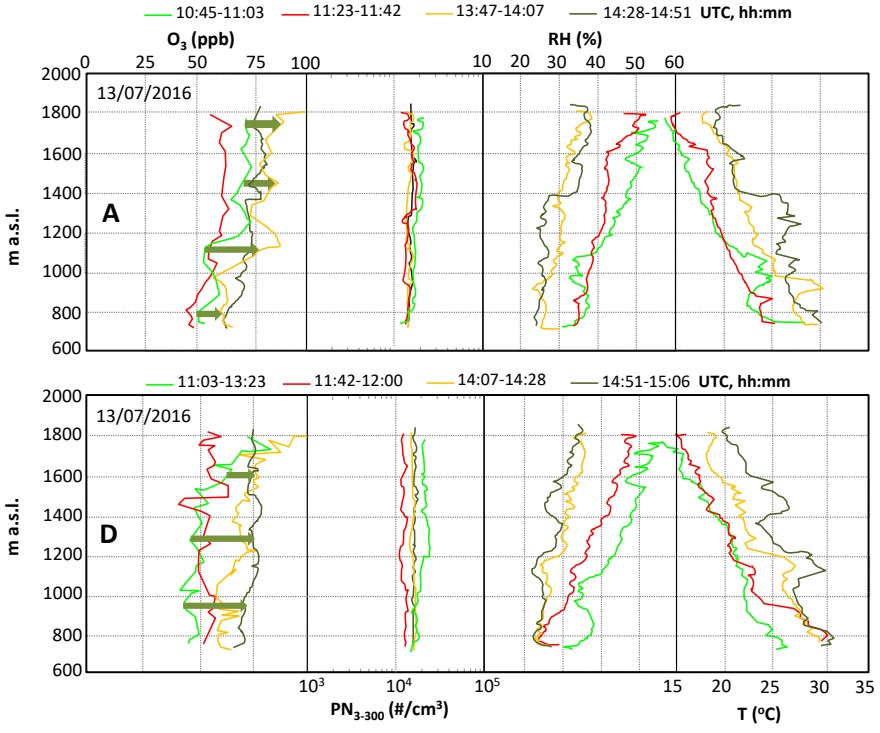

FIGURE 10

Atmos. Chem. Phys. Discuss., https://doi.org/10.5194/acp-2017-1014
Manuscript under review for journal Atmos. Chem. Phys.
Discussion started: 27 November 2017

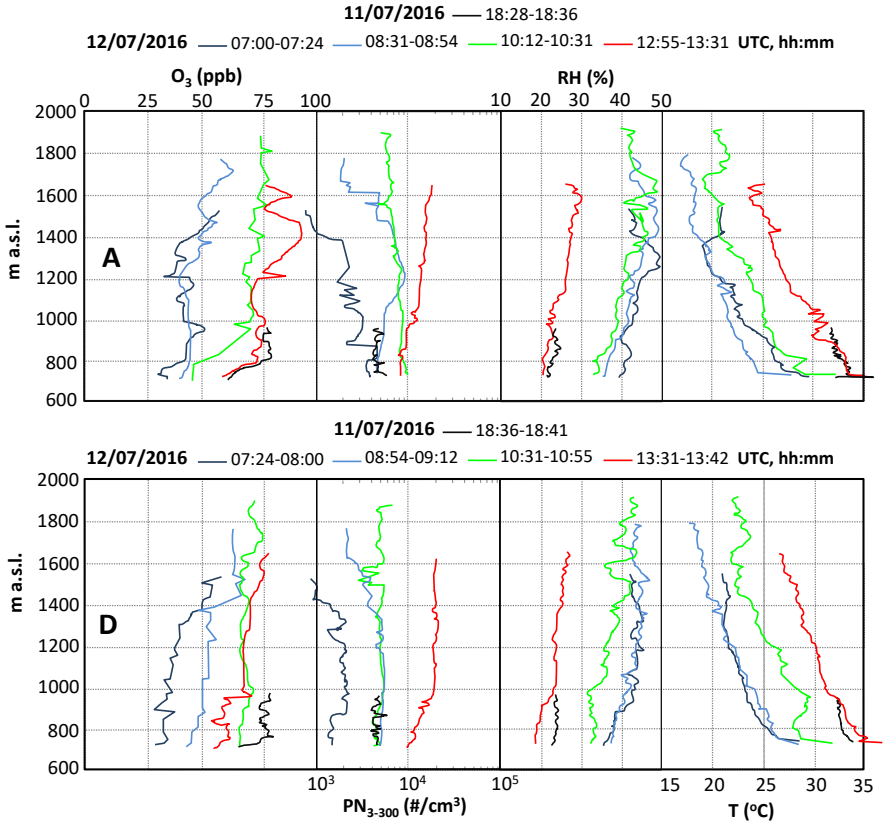

FIGURE 11

Atmos. Chem. Phys. Discuss., https://doi.org/10.5194/acp-2017-1014
Manuscript under review for journal Atmos. Chem. Phys.
Discussion started: 27 November 2017

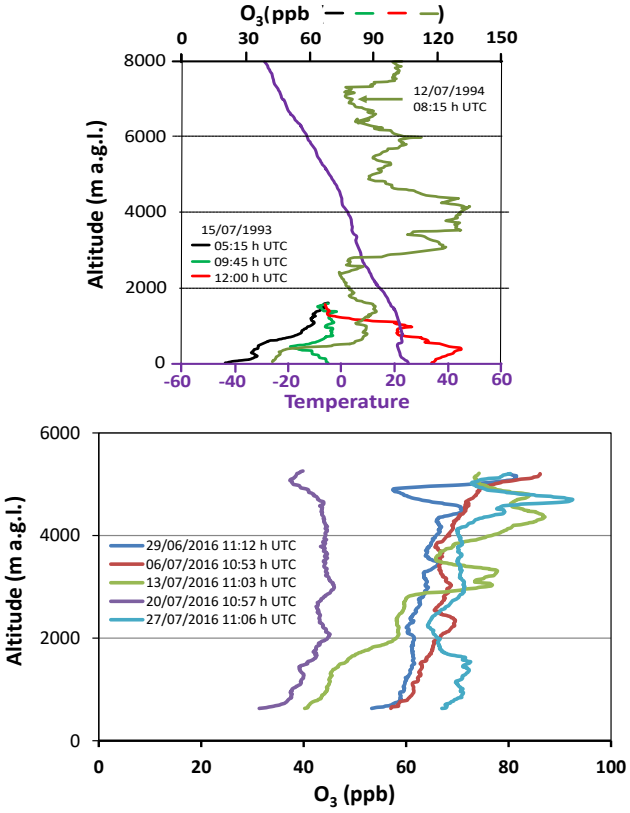

FIGURE 12

Atmos. Chem. Phys. Discuss., https://doi.org/10.5194/acp-2017-1014
Manuscript under review for journal Atmos. Chem. Phys.
Discussion started: 27 November 2017

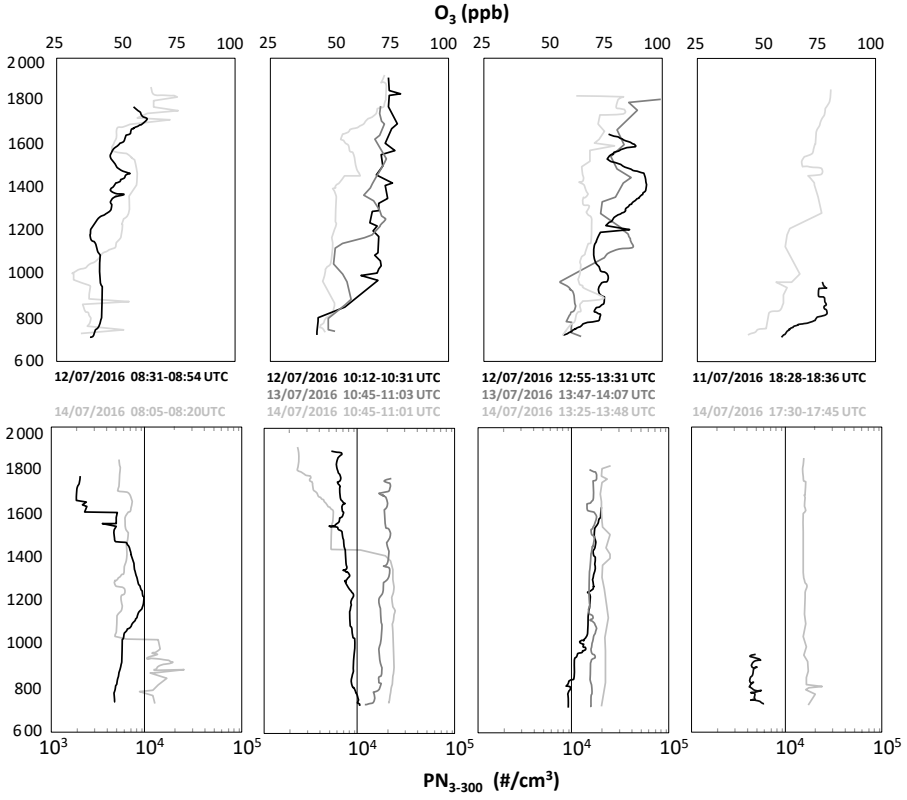

Figure 13

Atmos. Chem. Phys. Discuss., https://doi.org/10.5194/acp-2017-1014
Manuscript under review for journal Atmos. Chem. Phys.
Discussion started: 27 November 2017

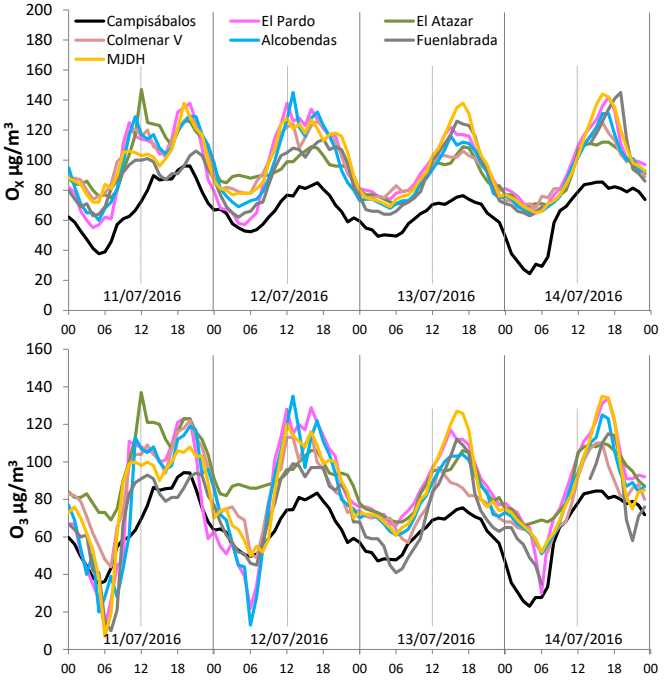

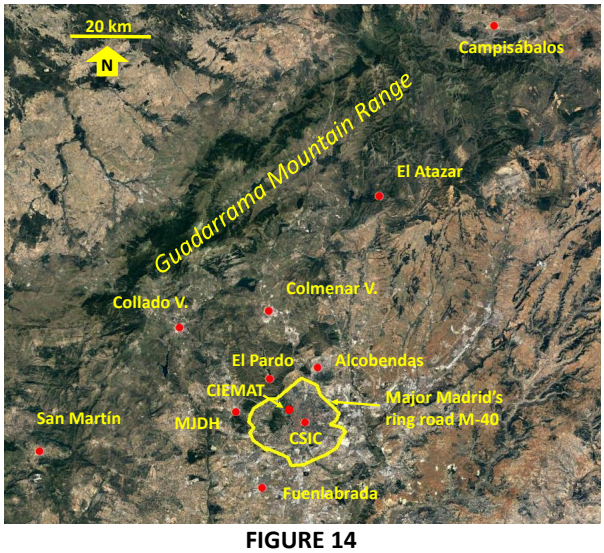

FIGURE 14

Atmos. Chem. Phys. Discuss., https://doi.org/10.5194/acp-2017-1014
Manuscript under review for journal Atmos. Chem. Phys.
Discussion started: 27 November 2017

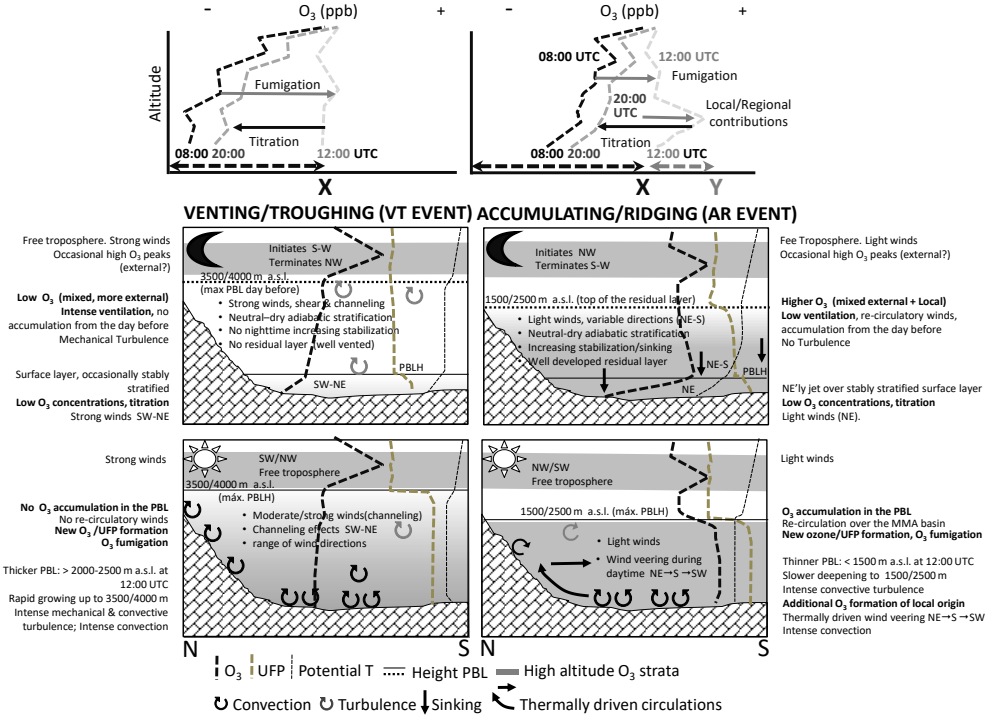

FIGURE 15

Atmos. Chem. Phys. Discuss., https://doi.org/10.5194/acp-2017-1014
Manuscript under review for journal Atmos. Chem. Phys.
Discussion started: 27 November 2017

912 **TABLES**

913 Table 1. Details of the instrumentation used in the three supersites and the platform mounted
914 on tethered balloons.

Site	Latitude (N)	Longitude (W)	Altitude (m a.s.l.)	Parameter (Device-Model)	Operation period
CSIC	40º26'25"	03º41'17"	713	NOx (Teledyne API 200EU) O3 (2B Technologies 202) UFP>2.5nm (CPC-TSI 3775) BC (Aethalometer-AE33) PM1 (OPC-GRIMM 1107)	09-20/07/2016
CIEMAT	40º27'23"	03º43'32"	669	NO_X (THERMO 17i) O_3 (THERMO 49i) UFP>7nm (CPC-TSI 3772) UFP>2.5nm (CPC-TSI 3776) BC (Aethalometer-AE33) PM2.5 (TEOM©) Meteorological tower	04-20/07/2016
ISCIII	40º27'27"	03º51'54"	739	NO_X (THERMO 17i) O_3 (THERMO 49i) UFP>7nm (CPC-TSI 3783) UFP>2.5nm (CPC-TSI 3776) BC (MAAP–THERMO) PM_1 (OPC-GRIMM 1108) PTR-ToF-MS (HR 8000, Ionicon)(operating procedures described in SI)	04-20/07/2016
MJDH-RC (vertical profiles)	40º28'30"	03º52'55"	729	UFP>3nm (CPC Hy-CPC) O_3 ($PO3M^{TM}$ 2B Technologies) Meteorology (Temp., RH, Press., wind speed and direction)	11-14/07/2016

915
916

Atmos. Chem. Phys. Discuss., https://doi.org/10.5194/acp-2017-1014
Manuscript under review for journal Atmos. Chem. Phys.
Discussion started: 27 November 2017

Atmospheric Chemistry and Physics Discussions

917 Table 2. Vertical measurement profiles obtained during 11-14/07/2016 at Majadahonda (MJDH-RC).
918

Day	Starting hour (UTC)	Final hour (UTC)	Number of profiles	Maximum height (m a.s.l.)
11/07/2016	18:30	18:45	2	200
12/07/2012	07:02	07:40	2	850
	08:30	09:10	2	1000
	10:10	10:56	2	1100
	11:55	13:43	2	900
13/07/2008	10:45	11:25	2	1000
	11:25	12:00	2	1000
	13:47	14:29	2	1000
	14:29	15:12	2	1100
14/07/2004	08:03	08:44	2	1150
	08:48	10:37	2	1100
	10:46	12:45	2	1200
	13:22	14:02	2	1100
	15:23	16:13	2	1025
	17:12	17:31	2	1100

919